

Influenza virus is a member of the *Orthomyxoviridae* family and is divided into Type A, B and C viruses. Type A influenza viruses are candidates for annual epidemic and occasional pandemics, and are sub-divided by hemagglutinin (HA) and neuraminidase (NA) [1]. Among the various types of HA, H1 and H3 subtypes are found in human and mutations in these enable the virus to evade the immune system. Recently, a highly pathogenic avian influenza A virus (H5N1) has been identified in poultry, migratory birds and human beings, which has resulted in severe disease or death around the world. As of August 16, 2007, there have been 321 confirmed human cases of avian influenza A (H5N1) reported to the WHO and 194 of these have died [2]. Although transmission from human to human is inefficient and limited, the virus has the potential to cause the next influenza pandemic, and it is essential to prepare for such a possible pandemic [3]. Among various strategies for dealing with this possibility, vaccination is the principal defense strategy for reducing morbidity and mortality during a pandemic. However, conventional split influenza vaccines might be unsuitable against a pandemic caused by influenza type H5N1. Thus, development of a pandemic influenza vaccine is urgently required. The Japanese Ministry of Health Labour and Welfare (MLHW) have released guidelines for fast-track licensing of pandemic influenza vaccine. During the pre-pandemic period, submission of a mock-up pandemic vaccine were formally assessed and approved by national regulatory authorities.

Several influenza vaccines are now being developed and pre-clinically and clinically assessed by several vaccine manufacturers around the world [4]. In clinical trials, an immune response is induced by two shots of high doses of an inactivated sub-virion vaccine based on H5N1 virus isolated in 2004 [5,6] and a recombinant hemagglutinin based on H5N1 virus isolated in 1997 [7]. To induce a high level of immunity after one dose, several countries have tried to develop a whole-virion vaccine. Whole-virion vaccines are more immunogenic than split-virion vaccines [8]; however the reactogenicity of whole-virion vaccines is higher than that of split vaccines [9]. A clinical trial in China clearly showed that antibody responses were well induced after the first dose, and that no serious adverse event was reported [10]. Despite the evidence that there are differences in immunogenicity and reactogenicity between whole and sub-virion vaccines, there have been few pre-clinical trials and animal safety tests. It is important to address whether pre-clinical and animal safety tests can predict and correlate to clinical trials [11], and a rapid and more sensitive safety test must be developed.

In Japan, the MLHW decided to develop and save whole-virion H5N1 vaccine adjuvanted with aluminum hydroxide. In Japan, as in other countries, all vaccines for human use must conform to the "Minimum Requirements for Biological Products" and are obliged to pass national control tests [12]. Quality control of influenza vaccines is performed by the abnormal toxicity test (ATT) and the leukopenic toxicity test (LTT), which are based on body weights and peripheral white blood cell (WBC) counts in mice after subcutaneous or intra-peritoneal injection [13,14]. However, it was not known whether these tests (ATT and LTT) could evaluate the safety of pandemic influenza vaccine, and these tests require a lot of animals and days. In addition, several researchers have discussed the safety of aluminum adjuvant-containing

influenza vaccines [15]. Although aluminum hydroxide is thought to be safe and has long been used as a vaccine adjuvant, aluminum adjuvants have resulted in macrophagic myofasciitis and delayed-type hypersensitivity [16]. Thus, we must investigate the safety and toxicity of whole-virion H5N1 vaccine adjuvanted with aluminum hydroxide.

In this study, we compare pandemic vaccine (PDv; whole-virion H5N1 vaccine adjuvanted with aluminum hydroxide), whole virion-particle vaccine (WPv) without any adjuvant, and HA vaccine (HAV). In addition, to develop rapid and more sensitive and reproducible methods, we performed a comprehensive gene expression analysis of rats after administration of the various type of influenza vaccine, using DNA microarrays. Our previous study clearly shows that cDNA microarrays are a useful technology with which to evaluate the safety and quality of pertussis vaccine, and we can successfully identify the genes related to vaccine toxicity [17]. In the present study, we developed the cDNA microarray technology and applied it to the safety evaluation of Influenza A/Vietnam/1194/2004 (H5N1) vaccines.

Materials and methods

Animals

Male Fisher-344 (F344) rats (8 weeks) were obtained from SLC (Tokyo, Japan). All animals were housed in rooms maintained at $23 \pm 1^\circ\text{C}$, with $50 \pm 10\%$ relative humidity, and 12-h light: 12-h dark cycles, at least 1 week prior to the test challenge. Rats typically weighed 160–200 g on arrival.

Vaccines

The following vaccines were used in this study. (1) PDv: inactivated monovalent A/H5N1 whole-virion influenza vaccine (derived from NIBRG-14: A/Vietnam/1194/2004) adjuvanted with aluminum hydroxide, containing $30 \mu\text{g}$ HA/ml. NIBRG-14 is constructed by reverse genetics, using A/Vietnam/1194/2004 and PR-8 (H1N1). (2) WPv: inactivated whole trivalent influenza vaccines (A/Newcaledonia/20/99 (H1N1), A/Hiroshima/52/2005 (H3N2), and B/Malaysia/2506/2004), containing $30 \mu\text{g}$ HA/ml each strain. (3) HAV: trivalent HA influenza vaccine (A/Newcaledonia/20/99 (H1N1), A/Hiroshima/52/2005 (H3N2), and B/Malaysia/2506/2004), containing $30 \mu\text{g}$ HA/ml each strain. All vaccines were produced and manufactured by The Chemo-Sero-Therapeutic Research Institute, Kaketsuken (Kumamoto, Japan). All vaccines complied with the minimum requirement for biological products in Japan. Each 5 ml vaccine was intra-peritoneally (*i.p.*) injected into rats. Five milliliters of saline (SA) (Otsuka normal saline; Otsuka Pharmaceutical Factory, Inc., Naruto, Tokushima, Japan) was intra-peritoneally injected as a control.

Abnormal toxicity test and leukopenic toxicity test

According to the minimum requirement for biological products in Japan [12], we performed an abnormal toxicity test and a leukopenic toxicity test for influenza vaccine (PDv,

WPv, HAv and SA). We used healthy rats showing no sign of disease and normal increases in body weight during a 7-day quarantine period before injection. Each 5 ml vaccine was intra-peritoneally (*i.p.*) injected into five rats. Five milliliters of saline was intra-peritoneally injected as a control. We checked the body weights of rats for 4 days. For the LTT, peripheral blood was collected from tail vein at 2, 16, 48, 72 and 96 h after virus vaccine injection. Immediately, we counted the number of peripheral blood leukocytes (PBL), mean corpuscular hemoglobin (HGB), red blood cells (RBC), hematocrit (HCT), mean corpuscular volume (MCV) and platelets (PLT), using an automatic haematocytometer, the Celltac MEK-5254 (Nihon Kohden, Tokyo, Japan). To assess the significance of differences, a *z*-test for ATT data and a Student's *t*-test for LTT data were performed according to the minimum requirements for biological products in Japan [12]. All statistical analyses were performed by GraphPad Prism (version 4, GraphPad Software, San Diego, CA).

Histology

Animals were anesthetized with diethylether and the brains, thymuses, lungs, livers, spleens, pancreases, small intestines, kidneys, testes and bone marrows were collected. Tissues were fixed with Bouin's solution (Sigma, St. Louis, MO) and 4% (w/v) paraformaldehyde in phosphate-buffered saline (PBS) for at 4°C for 24 h. After fixation, tissues were dehydrated through a series of graded ethanols and xylene and embedded in paraffin. Tissue samples were cut into 4 µm sections and stained with hematoxylin and eosin (H.E.). Five rats per group, treated with each vaccine, were analyzed on days 1–4 post-treatment.

RNA preparation

Animals treated with PDv, WPv, HAv and SA were anesthetized with diethylether and lung samples were collected. Lung samples were immediately frozen in liquid nitrogen for storage. Thawed tissue was homogenized and mixed with ISOGEN reagent (NIPPON GENE, Tokyo, Japan). Total RNA was prepared from lysates in accordance with the manufacturer's instructions. Poly(A)+RNA was prepared from total RNA using a Poly(A) Purist Kit (Ambion, Austin, TX), according to the manufacturer's instructions.

Microarray preparation and expression profile acquisition

For the microarray analysis, three lung samples from each rat were analyzed on days 1–4 post-treatment. In total 48 lung samples were analyzed in this experiment.

A set of synthetic poly-nucleotides (80-mers) representing 11,464 rat transcripts derived from 10,490 independent genes, and including most of the RefSeq clones deposited in the NCBI database (MicroDiagnostic, Tokyo, Japan), was arrayed on aminosilane-coated glass slides (Type I; Matsunami, Kishiwada, Japan) using a custom-made arrayer [18,19]. Poly(A)+RNA (2 µg) from each sample was labeled with Cyanine 5-dUTP (PerkinElmer, Boston, MA) using SuperScript II (Invitrogen, Carlsbad, CA); a common rat reference RNA (MicroDiagnostic) was labeled with Cyanine 3-dUTP (PerkinElmer, Boston, MA). Labeling, hybridization and washes of microarrays were performed using a Labeling & Hybridization Kit (MicroDiagnostic) according to the manufacturer's instructions. The rat common reference RNA was purchased as a single batch and labeled as an aliquot with Cyanine-3 for hybridization to a single microarray side by side with each sample labeled with Cyanine-5. Hybridization signals were measured using a GenePix 4000A scanner (Axon Instruments, Whipple Road Union City, CA) and then processed into primary expression ratios ([Cyanine 5-intensity obtained from each sample]/[Cyanine 3-intensity obtained from common reference RNA]), which are indicated as 'median of ratios' in GenePix Pro 3.0 software (Axon Instruments). Normalization was performed for the median of ratios (primary expression ratios) by multiplying normalization factors calculated for each feature on a microarray by the GenePix Pro 3.0 software.

Data analysis

Data processing and hierarchical cluster analysis were performed using Excel (Microsoft, Tokyo, Japan) and an MDI gene expression analysis software package (MicroDiagnostic). The primary expression ratios were converted into \log_2 values (\log_2 Cyanine-5 intensity/Cyanine-3 intensity) (designated log ratios) and compiled into a matrix (designated primary data matrix). To predict the most obvious differences obtained from cluster analysis of the primary data matrix, we extracted 5346 genes with \log_2 ratios over 1 or under -1 in at least one sample from the primary data matrix and subjected them to two-dimensional hierarchical cluster analysis for samples and genes. To identify genes demonstrating significant changes in expression, we undertook the following: (i) mean averages of \log_2 ratios were calculated for each gene from data sets of day 1 SA- and WPv-treated samples; (ii) standard deviations were calculated for each gene; (iii) the difference in mean averages between day 1 SA- and WPv-treated samples was calculated for each gene and divided by the sum of the corresponding standard deviation values. The difference in the mean averages/the sum of the standard deviations was defined as the signal-to-noise ratio for each gene. We chose the 76 genes

among PDv-, WPv-, HAv- and SA-treated animals 16 h after vaccine injection. Significant differences in body weight changes were observed between SA- and WPv-treated rats ($P < 0.01$), SA and PDv ($P < 0.01$). Increasing and decreasing rate in body weights are indicated as a percentage (%) compared to the body weight before injection; means \pm S.D. of five animals are shown. A significant difference in the numbers of platelets (center panel) and WBCs (right panel) was observed between SA- and WPv-treated rats ($P < 0.01$), as well as between SA- and PDv-treated rats ($P < 0.01$). (C) Histological analysis of vaccine-treated rat liver. Lung and kidney at day 1 after injection. Sectioned samples were stained with H.E. and analyzed at low (upper panel) and high (lower panel) magnification. NT, non-treatment; SA, saline; HAv, HA vaccine; WPv, whole particle vaccine and PDv, pandemic vaccine.

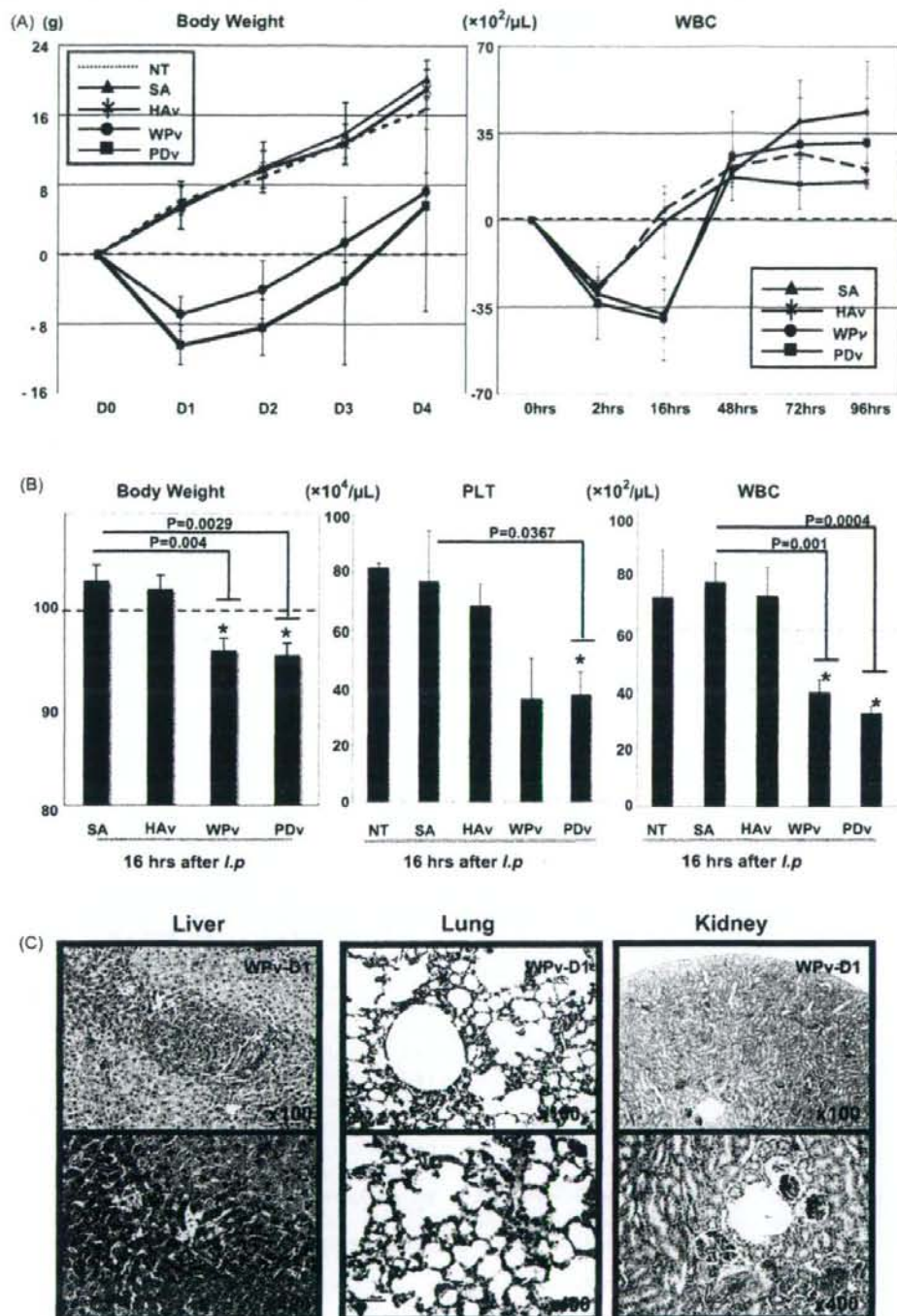


Figure 1 Influenza quality was evaluated by conventional National tests. (A) Abnormal toxicity test (left panel) and leukopenic toxicity test (right panel) for influenza vaccine (PDv, WPv, HAv, and SA). Body weight changes were plotted for 4 days (left panel). Changes in body weight are indicated by the mean increase \pm S.D. in five animals. The number of WBCs (white blood cells) was plotted for 4 days (right panel). Changes in WBCs are indicated by the mean increase \pm S.D. in five animals. (B) The differences

exhibiting the highest expression signal-to-noise indices and extracted expression data corresponding to these genes from the primary data matrix for all samples; this data was subsequently subjected to two-dimensional hierarchical cluster analysis for samples and genes.

Quantitative RT-PCR analysis

Changes of gene expression assessed by microarray analysis were confirmed by quantitative real-time reverse transcription-polymerase chain reaction (RT-PCR) for selected 18 genes. PCR primers (Table 2) were designed for 18 genes using the Primer Express software (Applied Biosystems, Foster City, CA). Poly (A) RNA was used to synthesize first strand cDNA using a First-strand cDNA Synthesis Kit (Life Science, Inc., St. Petersburg, FL), according to the manufacturer's instructions. Expression levels of selected genes were analyzed by quantitative (Q) reverse transcriptase-polymerase chain reaction using a 7500 Fast Real-Time PCR System (Applied Biosystems) with 7500 Fast System SDS Software Version 1.3. cDNA was amplified for Q-PCR using SYBR Green I (Molecular Probes, Inc.) to detect PCR product. One microliters of six-fold diluted cDNA was used in a 20- μ l final volume reaction containing 10 μ l SYBR Green[®] PCR Master Mix (Applied Biosystems), 0.2 μ M forward primer, and 0.2 μ M reverse primer. The 7500 Fast System was programmed to run an initial polymerase activation step at 95 °C for 10 min followed by 40 cycles of denaturation (95 °C for 15 s) and extension (60 °C for 1 min), and product synthesis was monitored at the end of the extension step of each cycle. Each expression values were normalized against rat Gapdh. Data presented in the Fig. 4 are the average and standard deviation of two independent quantitative RT-PCR analysis in each sample (SA, HAV, WPv and PDv). Statistical significance was calculated using Student's two-tailed *t*-test (paired two-sample for means) between WPv- and SA-treated rat lung. To determine the correlation between DNA microarray data and quantitative RT-PCR analysis, a Pearson correlation coefficient was calculated.

Results

Abnormal toxicity test for H5N1 influenza vaccine

Animals were treated with 5 ml of pandemic influenza vaccine (PDv; whole-virion H5N1 vaccine adjuvanted with aluminum hydroxide), whole virion-particle vaccine (WPv) without any adjuvant, HA vaccine (HAV) or saline as a control, and the body weight [BW] of each rat was checked at days 1, 2, 3 and 4. Five rats per group were analyzed each day after intraperitoneal (*i.p.*) injection of vaccine or saline. In SA- and HAV-treated animals, no decrease in the body weight (BW) was observed, and there were no significant differences in body weight changes between SA- and HAV-treated animals for 4 days (Fig. 1A). Decrease rate in BW was significantly different between PDv- and WPv-treated animals and SA- and HAV-treated rats, from 16 h to 4 days ($P < 0.05$) after injections (Fig. 1A and B). When we compared the decrease rate in BWs of PDv- and WPv-treated rats, no significant differences were observed between days

1 and 4. The abnormal toxicity test is a test that evaluates vaccine quality based on decreased body weights after *i.p.* injection to the animal in Japan. According to the criteria of the Japanese national regulatory test – Minimum Requirements for Biological Products [12], it can be concluded that vaccine quality in HAV is same as in the SA. However, vaccine quality in WPv and PDv were different from HAV and SA. In addition, within WPv and PDv, there was no significant difference in the vaccine quality.

Leukopenic toxicity test for various influenza vaccines

Animals were treated with 5 ml of PDv, WPv, HAV or SA as a control, and peripheral WBCs (white blood cells) were collected from tail veins at 2, 16, 48, 72 and 96 h after inoculation, and counted. Three rats per group, at each time point after sample *i.p.* injection, were analyzed. A reduction in WBC number was observed in all animals at 2 h after *i.p.* injection of SA, HAV, WPv and PDv. However, the decrease in the number of WBCs continued and a significant decrease in WBC number ($P < 0.05$) was observed in WPv- and PDv-treated animals, compared with SA- and HAV-treated animals, at 16 h after *i.p.* injection (Fig. 1A and B). In addition, a significant decrease ($P < 0.05$) in platelet (PLT) number was observed in WPv- and PDv-treated animals at 16 h after *i.p.* injection. No significant differences of the numbers of RBCs (red blood cells), HGB (mean corpuscular hemoglobin), HCT (hematocrit), or MCV (mean corpuscular volume) were observed among all groups (*data not shown*). According to the criteria of Japanese national regulatory test-Minimum Requirements for Biological Products [12], it can be concluded that vaccine quality in HAV is same as in the SA. However, vaccine quality in WPv and PDv were different from HAV and SA. In addition, within WPv and PDv, there was no significant difference in the vaccine quality.

Histological analysis of influenza vaccine-treated rats

Animals were treated with 5 ml of PDv, WPv, HAV or SA as a control, and various tissues (brain, thymus, lung, liver, spleen, kidney, testis, pancreas, and small intestine) were histologically evaluated. Among these tissues, focal necrosis (FN) of the liver was observed in the livers of both WPv- and SA-treated rats at day 1 after injection (Fig. 1C); after day 2, we could not detect any FN in the liver, indicating that FN was induced by experimental stress. No histopathological changes were observed in any other tissue.

Microarray analysis of vaccine-treated lung

To evaluate the effect of influenza vaccines on gene expression in the lung, we prepared three rats per group; PDv-, WPv-, HAV- and SA-treated groups were sacrificed and lung samples were taken at days 1, 2, 3 and 4. A total of 48 independent lung tissue samples were analyzed. We labeled poly(A)⁺ RNA purified from these samples and from a rat common reference RNA with Cyanine-5 and

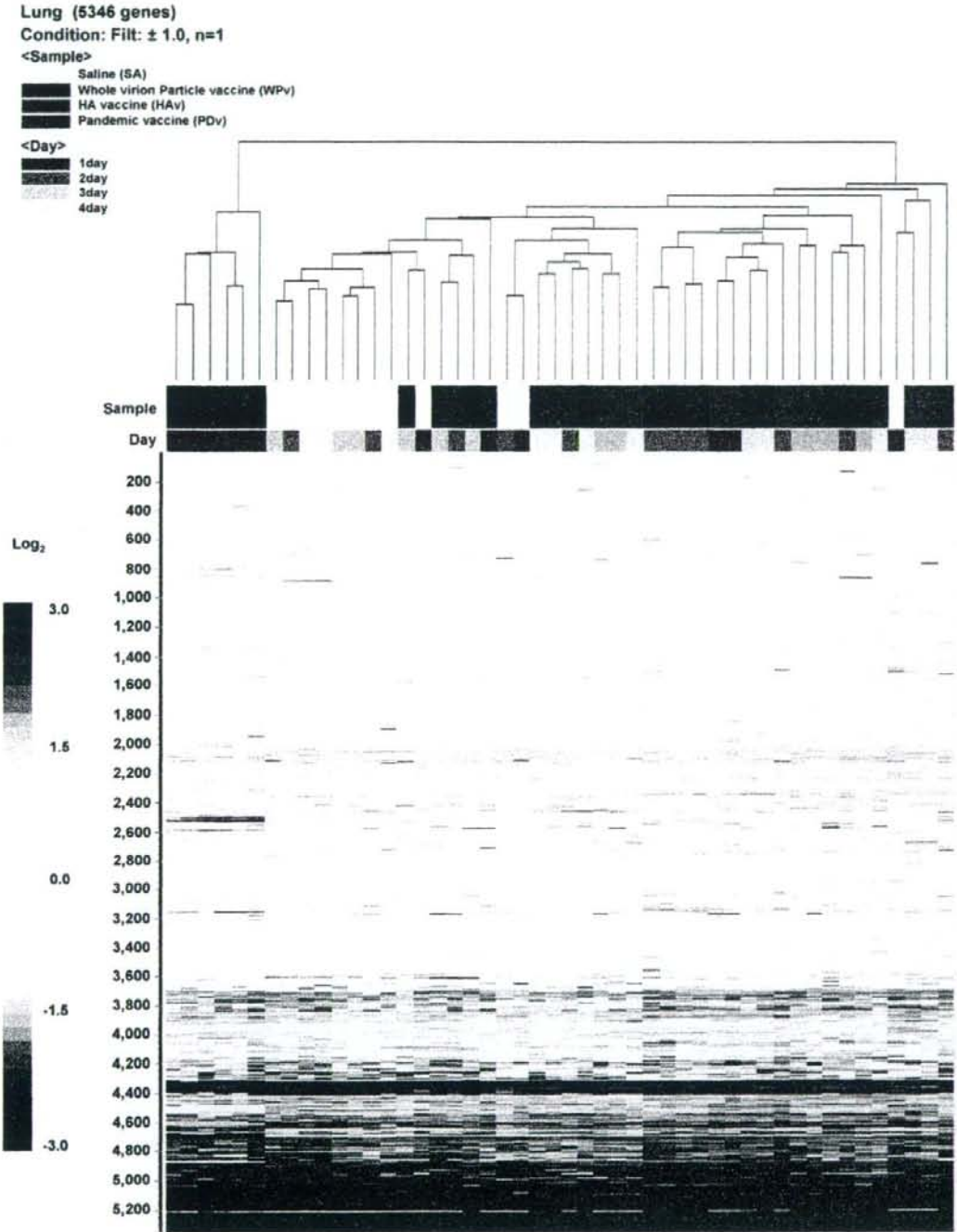


Figure 2 Overall gene expression profiles obtained from SA-, HAV-, WPv- and PDv-treated rat lung. Genes expressed in saline and vaccine-treated lungs are assembled in the order obtained from the results of cluster analysis. The color bar at the left shows the ratio vs the common reference RNA in log₂; red and blue indicate up and down-regulated genes, respectively. A matrix of 5346 genes that were up- or down-regulated in at least one experiment from day 1 to 4 after injection.

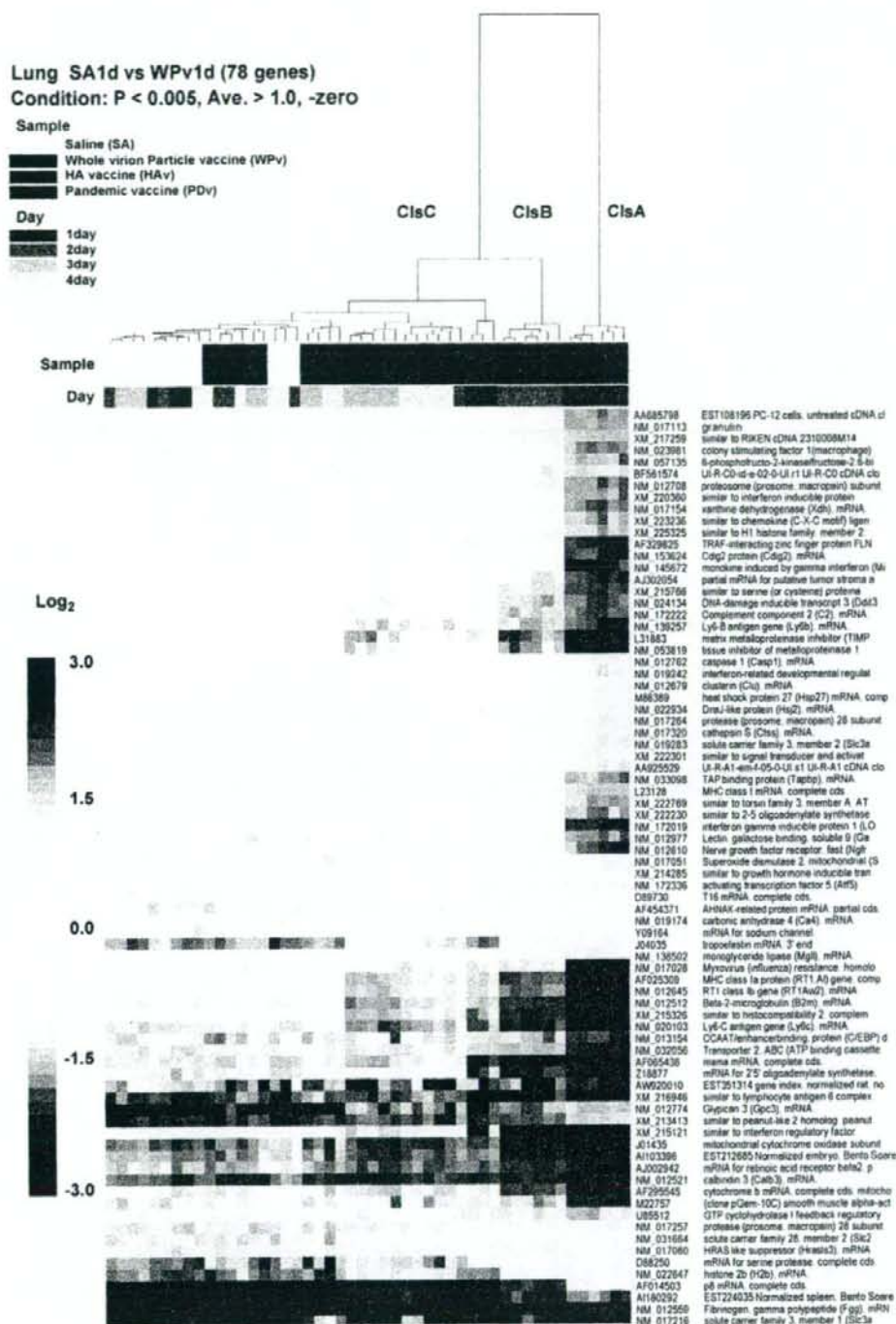


Figure 3 Microarray analysis of gene expression in the SA-, HAV-, WPV- and PDV- treated rat lung. A matrix of 76 genes regulated in at least one experiment from day 1 to 4 after injection. Hierarchical clustering of the 76 selected genes that were preferentially regulated in WPV-treated rat lung compared with SA-treated rat lung at day 1 ($P < 0.005$). ClsA, cluster A; ClsB, cluster B and ClsC, cluster C.

Table 1 Genes that were up- and down-regulated by influenza vaccine ($P < 0.005$)

Official gene name	Symbol	ID	PDV-D1 mean \pm S.D.	WPV-D1 mean \pm S.D.	HAV-D1 mean \pm S.D.	SA-D1 mean \pm S.D.
IFN-inducible gene						
Myxovirus (influenza virus) resistance 1	Mx1	X52711	6.163 \pm 0.276	5.514 \pm 0.19	2.198 \pm 0.272	0.935 \pm 0.117
Interferon regulatory factor 7	Irf7	XM.215121	5.39 \pm 0.67	5.51 \pm 0.39	2.06 \pm 0.87	0.32 \pm 0.08
Myxovirus (influenza virus) resistance 2	Mx2	NM.017028	4.08 \pm 0.13	3.83 \pm 0.06	1.14 \pm 0.41	-0.01 \pm 0.19
Interferon gamma inducible protein FLN29 gene product	Irf47	NM.172019	2.66 \pm 0.05	2.32 \pm 0.01	0.31 \pm 0.12	-0.06 \pm 0.12
Similar to interferon inducible protein	Fln29	AF329825	2.66 \pm 0.15	2.26 \pm 0.12	1.03 \pm 0.23	0.61 \pm 0.05
Interferon-related developmental regulator 1	Similar	XM.220360	1.84 \pm 0.23	1.74 \pm 0.06	0.61 \pm 0.15	0.45 \pm 0.05
	Ifrd 1	NM.019242	1.20 \pm 0.18	0.94 \pm 0.10	0.19 \pm 0.14	-0.26 \pm 0.12
Chemokine and cytokine function						
Lectin, galactoside-binding, soluble, 3 binding protein	Lgals3bp	AF065438	4.50 \pm 0.21	4.52 \pm 0.19	2.66 \pm 0.48	1.28 \pm 0.09
Tissue inhibitor of metalloproteinase 1	Timp1	NM.053819	2.75 \pm 0.12	2.66 \pm 0.22	0.78 \pm 0.39	-0.09 \pm 0.25
Chemokine (C-X-C motif) ligand 9	Cxcl9	NM.145672	2.54 \pm 0.52	2.88 \pm 0.13	0.78 \pm 0.18	0.35 \pm 0.15
Lectin, galactose binding, soluble 9	Lgals9	NM.012977	2.01 \pm 0.24	1.85 \pm 0.06	0.07 \pm 0.18	-0.65 \pm 0.20
Colony stimulating factor 1 (macrophage)	Csf1	NM.023981	1.94 \pm 0.07	1.81 \pm 0.24	0.84 \pm 0.13	0.59 \pm 0.16
Granulin	Grn	NM.017113	1.84 \pm 0.08	1.67 \pm 0.07	0.57 \pm 0.14	0.43 \pm 0.13
Chemokine (C-X-C motif) ligand 11	Cxcl11	XM.223236	1.70 \pm 0.37	1.60 \pm 0.14	1.32 \pm 0.09	0.21 \pm 0.07
EGF-containing fibulin-like extracellular matrix protein 1	Efemp1	D89730	0.28 \pm 0.18	-0.05 \pm 0.18	0.98 \pm 0.18	1.15 \pm 0.15
Immune response						
Similar to lymphocyte antigen 6 complex, Ly6-C antigen	Similar	XM.216946	4.83 \pm 0.19	4.58 \pm 0.11	2.96 \pm 0.23	2.25 \pm 0.23
Similar to histocompatibility 2, complement	Ly6c	NM.020103	3.75 \pm 0.11	3.33 \pm 0.26	1.89 \pm 0.41	1.44 \pm 0.08
RT 1 class Ib locus Aw2	Similar	XM.215326	3.67 \pm 0.20	3.51 \pm 0.05	1.68 \pm 0.44	0.74 \pm 0.06
Beta-2 microglobulin	RT1-Aw2	NM.012645	2.93 \pm 0.00	2.60 \pm 0.06	1.29 \pm 0.23	0.74 \pm 0.05
MHC class Ia protein (RT1.A1) gene, comp	β 2m	NM.012512	2.90 \pm 0.12	2.86 \pm 0.11	1.52 \pm 0.12	0.86 \pm 0.09
Lymphocyte antigen 6 complex, locus B	RT1-A1	AF025309	2.79 \pm 0.07	2.74 \pm 0.10	1.49 \pm 0.19	0.85 \pm 0.06
Transporter 2, ATP-binding cassette, sub-family B (MDR/TAP)	Ly6b	NM.139257	2.70 \pm 0.20	1.97 \pm 0.10	0.80 \pm 0.18	0.44 \pm 0.18
Complement component 2	Tap2	NM.032056	2.69 \pm 0.29	2.51 \pm 0.20	1.44 \pm 0.06	1.40 \pm 0.22
Proteasome (prosome, macropain) subunit, beta type 9	C2	NM.172222	2.07 \pm 0.10	2.00 \pm 0.21	0.93 \pm 0.09	0.31 \pm 0.09
TAP binding protein	Psmb9	NM.012708	2.07 \pm 0.13	1.73 \pm 0.01	0.48 \pm 0.05	0.21 \pm 0.07
RT1 class Ib gene, H2-TL-like, grc region (N3)	Tapbp	NM.033098	1.95 \pm 0.13	1.63 \pm 0.13	0.12 \pm 0.11	-0.10 \pm 0.10
Proteasome (prosome, macropain) 28 subunit, alpha	RT1-N3	L23128	1.62 \pm 0.03	1.45 \pm 0.20	0.14 \pm 0.16	-0.14 \pm 0.22
Cathepsin 5	Psme 1	NM.017264	1.20 \pm 0.10	0.79 \pm 0.01	0.06 \pm 0.11	-0.63 \pm 0.09
Complement component 1, s subcomponent	Ctss	NM.017320	0.99 \pm 0.12	0.59 \pm 0.17	0.03 \pm 0.08	-0.42 \pm 0.06
Proteasome (prosome, macropain) 28 subunit, beta	C1s	D88250	0.83 \pm 0.07	0.82 \pm 0.08	-0.93 \pm 0.16	-1.90 \pm 0.09
Elastin	Psme2	NM.017257	0.26 \pm 0.03	0.02 \pm 0.15	-0.78 \pm 0.23	-1.41 \pm 0.22
Fibrinogen, gamma polypeptide	Eln	J04035	0.01 \pm 0.21	0.08 \pm 0.26	1.95 \pm 0.11	1.83 \pm 0.25
	Fgg	NM.012559	-2.70 \pm 0.26	-2.78 \pm 0.22	-3.68 \pm 0.32	-3.80 \pm 0.21
Transcription activity						
Z-DNA binding protein 1	Zbp1	AJ302054	2.73 \pm 0.46	2.12 \pm 0.19	1.02 \pm 0.07	0.32 \pm 0.15
CCAAT/enhancer binding protein (C/EBP), delta	Cebpd	NM.013154	2.58 \pm 0.41	2.20 \pm 0.08	1.38 \pm 0.15	0.70 \pm 0.22

Table 1 (Continued)

Official gene name	Symbol	ID	PDv-D1 mean \pm S.D.	WPv-D1 mean \pm S.D.	HAv-D1 mean \pm S.D.	SA-D1 mean \pm S.D.
Similar to H1 histone family, member 2;	Similar	XM.225325	1.67 \pm 0.19	1.31 \pm 0.06	0.21 \pm 0.03	0.08 \pm 0.18
Activating transcription factor 5	Atf5	NM.172336	0.95 \pm 0.06	0.99 \pm 0.06	0.76 \pm 0.29	-0.74 \pm 0.03
AHNAK nucleoprotein (desmoyokin)	Ahnak	AF454371	0.58 \pm 0.21	0.36 \pm 0.18	0.85 \pm 0.11	1.36 \pm 0.17
Nuclear protein 1	Nupr1	AF014503	-0.74 \pm 0.11	-1.09 \pm 0.04	-2.78 \pm 0.28	-2.83 \pm 0.07
histone cluster 1, H2bl	Hist1h2bl	NM.022647	-0.95 \pm 0.07	-0.93 \pm 0.13	-1.77 \pm 0.06	-1.98 \pm 0.13
Apoptosis						
Caspase 1 (Casp1), mRNA.	Casp1	NM.012762	0.92 \pm 0.13	0.91 \pm 0.07	0.12 \pm 0.05	-0.34 \pm 0.17
Heat shock protein 27 (Hsp27) mRNA, comp	Hsp27	M86389	0.90 \pm 0.14	0.84 \pm 0.15	0.08 \pm 0.05	-0.20 \pm 0.14
Mitochondrial cytochrome oxidase subunits, I, II, III genes, 9		J01435	-3.51 \pm 0.27	-3.63 \pm 0.10	-1.89 \pm 0.16	-2.08 \pm 0.12
Protein modification						
Serine (or cysteine) peptidase inhibitor, clade G, member 1	Serping1	NM.199093	2.20 \pm 0.12	2.14 \pm 0.03	0.66 \pm 0.16	0.08 \pm 0.13
Cellular signaling						
DNA-damage inducible transcript 3	Ddit3	NM.024134	2.07 \pm 0.20	1.97 \pm 0.21	0.38 \pm 0.22	0.30 \pm 0.24
HRAS like suppressor 3	Hrasls3	NM.017060	0.98 \pm 0.18	0.46 \pm 0.11	-0.84 \pm 0.22	-1.23 \pm 0.18
Similar to signal transducer and activate	Similar	XM.222301	0.80 \pm 0.28	0.94 \pm 0.23	-0.15 \pm 0.08	-0.28 \pm 0.12
Retinoic acid receptor, beta	Rarb	AJ002942	-2.73 \pm 0.09	-2.81 \pm 0.21	-1.86 \pm 0.16	-1.61 \pm 0.22
Metabolism						
2',5'-Oligoadenylate synthetase 1, 40/46 kDa	Oas1	Z18877	4.27 \pm 0.41	4.14 \pm 0.30	1.96 \pm 0.60	1.38 \pm 0.43
Similar to 2-5 oligoadenylate synthetase	Similar	XM.222230	1.75 \pm 0.35	1.70 \pm 0.24	0.43 \pm 0.39	0.07 \pm 0.08
6-Phosphofructo-2-kinase/fructose-2,6-biphosphatase 3	Pfkfb3	NM.057135	1.72 \pm 0.36	1.62 \pm 0.16	0.99 \pm 0.16	0.47 \pm 0.19
Carbonic anhydrase 4	Ca4	NM.019174	-0.85 \pm 0.33	-0.84 \pm 0.12	0.66 \pm 0.15	0.66 \pm 0.15
Monoglyceride lipase	Mgl1	NM.138502	-0.90 \pm 0.03	-1.16 \pm 0.23	-0.43 \pm 0.05	-0.08 \pm 0.22
GTP cyclohydrolase I feedback regulator	Gchfr	U85512	-1.24 \pm 0.09	-1.65 \pm 0.11	-1.22 \pm 0.21	-0.49 \pm 0.22
Cytochrome b mRNA, complete cds; mitocho	cytb	AF295545	-2.55 \pm 0.19	-2.65 \pm 0.11	-1.17 \pm 0.06	-1.30 \pm 0.14
Others						
EST351314 gene index, normalized rat, no	EST	AW920010	2.96 \pm 0.48	2.42 \pm 0.18	2.02 \pm 0.48	1.41 \pm 0.23
Nerve growth factor receptor (TNFR superfamily, member 16)	Ngfr	NM.012610	2.62 \pm 0.30	1.85 \pm 0.31	-0.25 \pm 0.43	-0.59 \pm 0.17
Cdig2 protein	Cdig2	NM.153624	2.62 \pm 0.11	2.08 \pm 0.09	0.70 \pm 0.17	0.46 \pm 0.06
Xanthine dehydrogenase	Xdh	NM.017154	2.02 \pm 0.11	1.95 \pm 0.16	0.77 \pm 0.04	0.47 \pm 0.28
EST108196 PC-12 cells, untreated cDNA cl	EST	AA685798	1.92 \pm 0.11	1.69 \pm 0.07	0.54 \pm 0.07	0.30 \pm 0.10
Similar to torsin family 3, member A; AT	Similar	XM.222769	1.76 \pm 0.08	1.48 \pm 0.35	0.02 \pm 0.38	-0.14 \pm 0.20
Glypican 3	Gpc3	NM.012774	1.61 \pm 0.08	1.46 \pm 0.23	2.62 \pm 0.57	2.71 \pm 0.13
Similar to RIKEN cDNA 2310008M14 [Mus mu	Similar	XM.217259	1.58 \pm 0.02	1.55 \pm 0.14	0.58 \pm 0.20	0.13 \pm 0.04
Similar to peanut-like 2 homolog; peanut	Similar	XM.213413	1.38 \pm 0.15	1.33 \pm 0.07	2.20 \pm 0.18	2.33 \pm 0.09
Solute carrier family 3 (activators of dibasic and neutral amino acid transport), member	Slc3a2	NM.019283	1.21 \pm 0.13	0.75 \pm 0.07	-0.14 \pm 0.28	-0.38 \pm 0.6
UI-R-A1-em-f-05-0-UI.s1 UI-R-A1 cDNA clo	EST	AA925529	1.15 \pm 0.13	0.82 \pm 0.07	-0.06 \pm 0.15	-0.54 \pm 0.14

Table 1 (Continued)

Official gene name	Symbol	ID	PDv-D1 mean \pm S.D.	WPv-D1 mean \pm S.D.	HAv-D1 mean \pm S.D.	SA-D1 mean \pm S.D.
Superoxide dismutase 2, mitochondrial	Sod2	NM_017051	0.86 \pm 0.09	0.60 \pm 0.11	-0.77 \pm 0.35	-1.04 \pm 0.04
Clusterin	Clu	NM_012679	0.78 \pm 0.09	0.74 \pm 0.09	-0.21 \pm 0.16	-0.37 \pm 0.16
DnaJ (Hsp40) homolog, subfamily A, member 1	Dnaja1	NM_022934	0.72 \pm 0.16	0.66 \pm 0.12	-0.26 \pm 0.09	-0.42 \pm 0.10
Similar to growth hormone inducible tran	Similar	XM_214285	0.49 \pm 0.08	0.26 \pm 0.17	-0.47 \pm 0.25	-0.80 \pm 0.09
Solute carrier family 28	Slc28a2	NM_031664	0.16 \pm 0.16	0.01 \pm 0.09	-0.71 \pm 0.26	-1.15 \pm 0.19
Sodium channel, voltage-gated, type VII, alpha	Scn7a	Y09164	-0.39 \pm 0.25	-0.48 \pm 0.14	0.09 \pm 0.41	0.54 \pm 0.03
EST224035 Normalized spleen, Bento Soare	EST	AI180292	-2.20 \pm 0.34	-1.64 \pm 0.20	-4.02 \pm 0.30	-2.94 \pm 0.25
smooth muscle alpha-actin	Acta2	M22757	-2.77 \pm 0.24	-2.34 \pm 0.09	-1.18 \pm 0.25	-1.17 \pm 0.05
Solute carrier family 3, member 1	Slc3a1	NM_017216	-3.10 \pm 0.66	-3.56 \pm 0.21	-2.92 \pm 0.65	-2.40 \pm 0.23
S100 calcium binding protein G	S100g	NM_012521	-3.93 \pm 0.29	-3.72 \pm 0.22	-2.17 \pm 0.15	-2.10 \pm 0.18

Cyanine 5-labeled lung RNA and Cyanine 3-labeled rat common reference RNA were competitively hybridized to a DNA microarray. Hybridization signals were processed into primary expression ratio ([Cyanine5-intensity obtained from each sample]/[Cyanine5-intensity obtained from each sample]), and normalized (primary expression ratio). The primary expression ratios were converted into \log_2 values (\log_2 Cyanine5-intensity/ \log_2 Cyanine5-intensity). \log_2 values for each sample were averaged and S.D. values were calculated. SA, Saline; HA, HA vaccine; WPv, whole particle vaccine, PDv, pandemic vaccine.

Cyanine-3, respectively. Next, we hybridized labeled RNAs to microarrays representing 11,464 transcripts derived from 10,490 independent genes, including most of the RefSeq clones deposited in the NCBI database. Hybridization signals were processed into expression ratios as \log_2 values (designated \log_2 ratios). To predict the most obvious differences obtained from cluster analysis of the primary data matrix, we extracted 5346 genes with \log_2 ratios over 1 or under -1 in at least one sample from the primary data matrix. When we performed a cluster analysis for 5346 tran-

scripts, two large clusters were obtained, and whole-virion vaccines (1 day after PDv- and WPv-treated) showed different clusters from the others (HA and SA) (Fig. 2). To evaluate the differences in gene expression between those induced by whole-virion vaccines and those induced by others (HA and SA), we extracted 76 genes essential for class separation ($P < 0.005$). When we performed a cluster analysis of these 76 genes, three large clusters were obtained. These 76 genes can distinguish whole-virion vaccines (PDv- and WPv-treated samples (day 1 and day 2)) from the oth-

Table 2 List of primers used in this study

Gene ID	Gene symbol	Forward primer	Reverse primer
NM_012512	β 2m	TTGAGCTACTGAAGAATGGAAAGAAGA	GGTGGGTGTAATTCAGTGTGA
NM_172222	C2	TTGTGCCTAGGGACTTCCACAT	GGCAAAAAGTCGAGGACACCAT
NM_145672	Cxcl9	TTTGCCCCAAGCCCTAACTG	TGGGTCTAGGCAGGTTTGATCTC
AF329825	FLN29	CCGGAGGAAGTCTCATTGA	GAAAGCTGCCAGTATTGAGTGAAC
XM_215121	Irf7	TGCAGCGTGAGGGTGTGTC	TCATCGTAGAGACTATTGGTCTAGACA
AF065438	Lgals3bp	TCTACCTCACCACTCCACTGACA	CAGGCTGCTGGAGGTTCTCT
NM_172019	Ifi47	CCTAGCCAACCAAGAAATGAATT	GGGAGTTTGGTGAAGGACAA
NM_019242	Ifrd1	GCAGTACCCTTGCAGACAAATGAAT	AAGTGTTCAGCATCGAGCATC
L23128	RT1-N3	AGTGGCTTCTGTCTGGCATTCT	AATGAGGTGTGAGAGGATGGAG
NM_017028	Mx2	AAGGAACATAGTGACACAGTGAGAAG	GGACAGGGCCAGCTTAACCA
NM_012708	Psmb9	CTCTGGCCATGAACCGAGAT	CAGCTCGTCTCCAGGATGA
NM_017264	Psmc1	ATCTATTGAGCCCCCTCTCTCGTT	GGGTGCAGTCTAGAGTTCTAGTCA
AF025309	RT1-A1	CCTGCGCTGTGTTCCCTTCCA	CAAGGAGTGACAGGATGCAGATGT
NM_012645	RT1-Aw2	TGCCGTGAGCCCCCTTCC	CCACAGCTCAAGAACAACAGAA
XM_223236	Cxcl1	CTGAAGGCTCATAAAGGACAAAGGT	CACATGTTCTGGCCCTTAA
NM_033098	Tapbp	GACCGTCCCAAAGACGAAAAG	TGGAGTCGTTTGACCAGAGAT
NM_053819	Timp1	CCTGTTACAGCCATCCCTTGC	GCCCTCAGAGCCCATGA
AJ302054	Zbp1	TTAGTAGTACCCCCAGAGTCAA	ACCTACGGTGGATGGTCTCTT
NM_017008	Gapdh	GTGAAGCTCATTTCTGGTATGACA	TTCTTACTCCTTGGAGGCCATGTAG

ers (HAv and SA) (Fig. 3). The three clusters formed by these 76 genes include: cluster A, whole virion-treated lung at day 1; cluster B, whole virion-treated lung at day 2; and cluster C, sub-virion and SA-treated rat lung at day 1. These 76 genes are listed in Table 1. Among these 76 genes, we found that the genes up-regulated by influenza infection included interferon-stimulated genes (ISGs), such as *Mx1* (myxovirus (influenza virus) resistance 1), *Irf47* (interferon gamma inducible protein 47), *Ifrd1* (interferon-related developmental regulator 1), *FLN29* (FLN29 gene product) and *Cxcl9* (chemokine (C-X-C motif) ligand 9), as shown in Table 1. In addition, genes up-regulated by the immune response and antigen presentation, including *Ctss* (cathepsin S), *Psme1* (proteasome (prosome, macropain) 28 subunit, alpha), *Psme2* (proteasome (prosome, macropain) 28 subunit, beta), *Tap2* (transporter 2, ATP-binding cassette, sub-family B (MDR/TAP)), *Tapbp* (TAP binding protein) *RT1-Aw2* (RT1 class Ib, locus Aw2), *RT1-N3* (RT1 class Ib gene, H2-TL-like, grc region (N3)) and $\beta 2m$ ($\beta 2$ microglobulin), were also strongly induced in whole-virion-treated rat lung.

To confirm and validate our DNA microarray analysis, we selected subset of 18 genes (Table 2), and performed quantitative RT-PCR analysis. Data presented in the Fig. 4 are the average, standard deviation and correlation between two independent quantitative RT-PCR and DNA microarray analysis in each sample (SA, HAv, WPv and PDv). As a result of comparison between two detection methods, Pearson's correlation coefficient indicates a statistically significant correlation between DNA microarray and quantitative RT-PCR analysis among our selected 18 genes. This correlation demonstrates excellent concordance between two methods. In addition, significant difference between WPv and SA was also observed in quantitative RT-PCR analysis ($P < 0.05$ [Student *t*-test]), similar to DNA microarray analysis.

These data suggest that vaccine quality in WPv and PDv were different from HAv. In addition, within WPv and PDv, there was no significant difference in the vaccine quality using DNA microarray analysis. Thus, it can be concluded that cDNA microarray technology is an informative, rapid and highly sensitive method with which to evaluate the

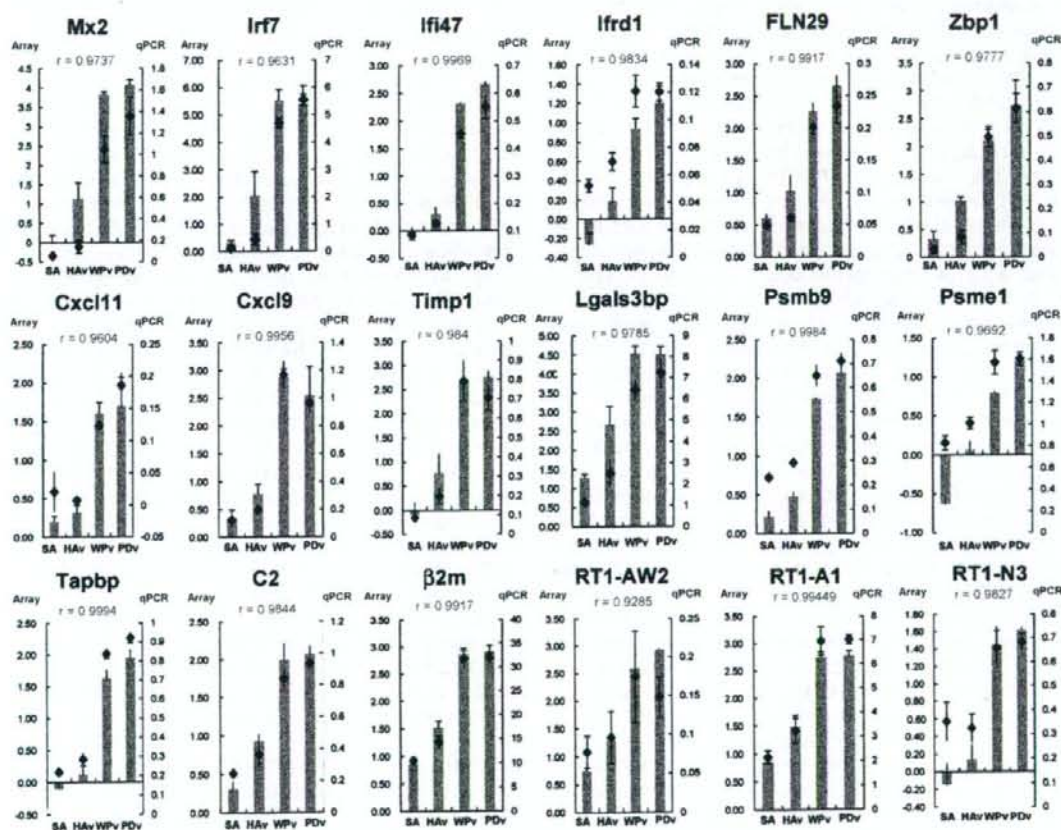


Figure 4 Comparison of cDNA microarray and quantitative real-time-PCR analysis. Expression of selected 18 genes from DNA microarray analysis (bar) is compared with real-time quantitative PCR data (dot) within the same pareto graph. Bar represented relative \log_2 ratios (average \pm S.D.) that extracted from the secondary data matrix for each selected genes (left side). Dot represented expression level (average \pm S.D.) of selected genes relative to rat β -actin derived from two independent quantitative RT-PCR analysis (right slide). A Pearson correlation coefficient was shown within each pareto graphs. Significant correlation between DNA microarray and quantitative PCR analysis was observed in our selected genes.

quality of influenza vaccines. Using DNA microarray system, consistent with the results of the ATT and LTT, there was no difference in global gene expression in the lung between PDv and WPv.

Discussion

Recently, quality assurance of the vaccines was rigorously controlled according to the good manufacturing practices (GMP), process validation, inspection and tests of the national regulator authority (NRA) in Japan and similar bodies in other countries. Current quality control and safety tests, such as the abnormal toxicity test and the leukopenic toxicity test, are useful to evaluate influenza vaccine safety for 50 years. ATT (also known as the general safety test or innocuity test) is a test for extraneous toxic contaminants in other countries. However, in Japan, the ATT is an established test that can evaluate vaccine quality based on changes in body weight over a period of 7 days after inoculation of final container vaccine compared to the trend data from past quality control test, statistically. These trend data was constructed at least 100 lot of each vaccine, which have already passed by the ATT and for which safety has been determined after post marketing surveillance. Whereas the ATT is a useful and long-performed test, the mechanism of the ATT was not well defined until recently [17]. In addition, inherent toxicity of vaccines and the intra-peritoneal injection route have been raised. For this reason, the relevance of the ATT has been questioned by some regulatory authorities. Currently, the FDA is discussing whether to abolish the requirement for the ATT, and the EMEA (European Agency for the Evaluation of Medicinal Products) has already decided to abolish the ATT for testing vaccines for human use.

In this study, we developed a new quality control method for influenza vaccine using DNA microarrays. We successfully translated the vaccine quality, immunogenicity and reactogenicity of influenza vaccine into gene expression profile data. According to the ATT, decrease in the body weight was only observed in whole virion-treated rats, and these tests did not distinguish PDv from WPv. Giving the same results as the ATT, the LTT showed that whole virion is different from sub-virion influenza vaccine, and there is no difference in vaccine quality between PDv and WPv. In the DNA microarray system, consistent with the results of the ATT and LTT, whole virion-treated rat lung was located in a different cluster from sub-virion- and SA-treated rat lung. Using gene expression profiles, we could not distinguish PDv from WPv. These data suggest that the DNA microarray system is not only equivalent to the ATT and LTT, but is also more informative. More interestingly, intra-peritoneal injection of influenza vaccine induced gene expression related to the immune response in a manner to be described below. These data predict that ATT and LTT are useful to evaluate the immunogenicity and reactogenicity, and intra-peritoneal injection can induce normal immunity. Moreover, using the DNA microarray system, the effect of vaccine treatment could be determined and substituted by gene expression profile changes.

In general, quality of gene expression data obtained from cDNA microarray has varied with platform and procedures used and validation of cDNA microarray should

be required for eliminate the effect of dye biases [20]. Our cDNA microarray method have been performed and validated by several different researchers, samples and condition [21–24]. In previous report, we performed two independent experiments of cDNA microarray and they are validated with another method of real-time PCR and *in situ* hybridization [17]. Real-time PCR is often referred to as a gold standard for gene expression measurement and validation of DNA microarray [25]. As a result of our validation, we have shown that there is a strong correlation between cDNA microarray and real-time-PCR analysis. These reports suggest that our cDNA microarray method have high reproducibility, reliability for the vaccine quality control. In this study, we have designed our experiment in same way of our previous research and also done real-time PCR analysis for 18 genes and yield statistically significant correlation between cDNA microarray and real-time PCR. These data have suggested that our cDNA microarray method for evaluating vaccine quality is reliable and validated.

Based on the changes in the expression profiles of 76 genes, we can distinguish whole-virion influenza vaccine (PDv: pandemic influenza vaccine and WPv: whole particle vaccine) from sub-virion vaccine (HAV: HA vaccine) and saline (Fig. 3). Among the 76 genes we extracted, we found that some genes were already reported as the endemic and pandemic influenza virus infection-inducing genes. The most common gene that influenza infection and vaccination induced was *Mx1* (myovirus (influenza virus) resistance 1). *Mx1* is an IFN-stimulated gene (ISG) and is induced by interferon (IFN) in many species. Some Mx GTPases have antiviral activity against a wide range of RNA viruses, including influenza viruses and members of the bunyavirus family [26]. Human influenza (H1N1 A/Texas/36/91) infection in lung [27] and 1918 pandemic influenza virus infection in bronchi [28] both induced MX (homologue of murine *Mx1*) genes, as shown by cDNA microarray analysis in Macaques. In the human middle ear epithelial cells, infection with influenza A/Alaska (6/77) (H3N2) also induced *Mx1* [29]. In our experiment, *Mx1* expression was highly induced in whole-virion influenza vaccine-treated rat lung, but not in sub-virion vaccine-treated rat lung. These data suggest that *Mx1* is one of the most promising biomarkers with which to evaluate influenza vaccine quality, and whole-virion vaccines have the same immunogenicity as influenza infection in the lung.

Similar to the influenza infection, other ISGs, *Irf47* [30], *Irfd1 FLN29* [31], and the gamma interferon-induced monokine *Cxcl9* (chemokine (C-X-C motif) ligand), were up regulated in whole-virion influenza vaccine-treated rat lung (Table 1). *Cxcl9* was induced by influenza infection in primary human umbilical vein endothelial cells (HUVECs) [32]. *Cxcl9*, which is a ligand of *Cxcr3*, stimulated the directional migration of activated CD8+ T cells to the lung, and contributed significantly to the accumulation of cytotoxic T lymphocytes (CTL) in the lung [33]. In addition, in the first case of H5N1 influenza infection in January 2003, patients with H5N1 disease had unusually high serum concentrations of *Cxcl9* and *IP-10* [34]. These data strongly suggest that whole-virion influenza vaccine induces proinflammatory cytokines like influenza A (H5N1) infection, and that *Cxcl9* is a common molecule related to influenza pathology and toxicity.

Among our extracted 76 genes, antigen modification and presentation-related genes, including *Ctss* (cathepsin S), *Psme1* (proteasome (prosome, macropain) 28 subunit, alpha), *Psme2* (proteasome (prosome, macropain) 28 subunit, beta), *Tap2* (transporter 2, ATP-binding cassette, sub-family B (MDR/TAP)), *Tapbp* (TAP (transporter associated with antigen processing)-binding protein), *RT1-Aw2* (RT1 class Ib, locus Aw2), *RT1-N3* (also known as MHC class I) and $\beta 2m$ (beta2-microglobulin), were up-regulated in PDV- and WPV-treated rat lung. *Tapbp* has an affinity to bind *Tap2*, which is a member of the family of ABC transporters and transports peptides from the cytosol into the endoplasmic reticulum for binding to MHC class I and $\beta 2m$ complex molecules for subsequent viral antigen presentation [35]. *RT1-Aw2* and *RT1-N3* form a MHC complex and $\beta 2m$ enhances the MHC stability and antigenicity of suboptimal CTL epitopes. These four genes have a major role of antigen presentation to CD8-T cells [36]. These data suggest that whole-virion vaccine more strongly induced CTL than sub-virion vaccine. These evidences support that whole-virion influenza vaccines have high immunogenicity than HA vaccine, and our method can potentially evaluate the effectiveness and efficacy of the vaccine by monitoring the expression of these genes. Further analyses are required whether these genes expression correlated to the antibody response and efficacy of influenza vaccine.

Among our screened genes, *Timp1* is induced by whole-virion influenza vaccine. *Timp1* (tissue inhibitor of metalloproteinase 1) is a member of the physiological inhibitors of matrix metalloproteinases (MMPs) and is produced in the respiratory tract on the development of airway inflammation and remodeling in the lung [37]. Recently, it was proposed that an imbalance between serum MMP-9 and TIMP-1 damages the blood-brain barrier and promotes febrile seizures or encephalopathy in cases of influenza virus infection [38]. These data suggest that *Timp1* up-regulation could be a possible phenotypic marker of toxicity related to encephalopathy. Acute disseminated encephalomyelitis (ADEM) and Guillain-Barre Syndrome (GBS) are both observed in 10–20 cases per 1 million adults and are most important issue in influenza vaccine safety [39]. In the United States, it was reported that highest number of GBS cases occurred in patients receiving an influenza vaccine followed by hepatitis vaccine [40]. Our data help us to understand the mechanism of adverse event in the vaccine injection. Further analysis will be required to determine whether up-regulation of these genes was observed in a particular lot of influenza vaccine, resulting in encephalopathy.

The most concerning matter is whether safety of aluminum adjuvanted pandemic influenza vaccine can be evaluated or not in this system. Using current quality control tests, such as the ATT, LTT and even more histological analysis, there was no significant difference in vaccine quality between PDV- and WPV-treated rats at any time point (Fig. 1A and C). In the DNA microarray system, there was no difference between PDV- and WPV-treated rats. These data strongly suggest that the vaccine quality of whole-virion vaccine with or without aluminum hydroxide were unchanged in the lung. These data might be helpful to understand the safety of aluminum hydroxide. More interestingly, it has been proposed that strain is a key factor in the influenza

vaccine. Comparing H5N1 and H1N1, no difference in vaccine quality was observed using DNA microarray analysis. These data strongly suggest that strain differences do not affect vaccine basal quality and that the type of vaccine, whether whole virion or sub-virion, is a main issue to induce high immunity if the influenza type for vaccine production matched to endemic or pandemic influenza infection.

Thus, it may be concluded that cDNA microarray technology is an informative, rapid and highly sensitive method with which to evaluate endemic and pandemic influenza vaccine quality. These findings suggest that our new method have a potential to shorten the time for the safety tests and can reduce the number of animals used. In addition, our test may contribute to the development of urgently required vaccine. Further analyses are required to confirm these gene expression changes correlate to the vaccine quality. At any rate, in terms of sensitivity and the amount of information available from one animal test, this method may be even better than current safety tests.

We previously reported several pertussis vaccine toxicity-related genes and proposed DNA microarray analysis as a new model for quality control tests [17]. In this study, we again proposed that DNA microarray analysis have a potential for the quality control of pandemic and endemic influenza vaccines.

Acknowledgements

We are grateful to Dr. Masato Tashiro, National Institute of Infectious Diseases, Japan for our research coordination and constructive discussion. The authors thank Dr. Hiroshi Yoshikura for helpful discussion and critical reading of the manuscript. *Funding:* This work was supported by Grants-in-Aid from Ministry of Health, Labour and Welfare, Japan.

References

- [1] Lamb RA, Krug RM. Orthomyxoviridae: the viruses and their replication. In: Knipe DM, Howley PM, editors. *Fields virology*. New York: Lippincott-Raven Press; 2000. p. 1487–531.
- [2] WHO website. http://www.who.int/csr/disease/avian_influenza/country/cases.table_2007_06_29/en/index.html.
- [3] Ungchusak K, Auewarakul P, Dowell SF, Kitphati R, Auwanit W, Puthavathana P, et al. Probable person-to-person transmission of avian influenza A (H5N1). *N Engl J Med* 2005;352(4):333–40.
- [4] Stephenson I, Gust I, Pervikov Y, Kieny MP. Development of vaccines against influenza H5. *Lancet Infect Dis* 2006;6(8):458–60.
- [5] Treanor JJ, Campbell JD, Zangwill KM, Rowe T, Wolff M. Safety and immunogenicity of an inactivated subvirion influenza A (H5N1) vaccine. *N Engl J Med* 2006;354(13):1343–51.
- [6] Bresson JL, Perronne C, Launay O, Gerdil C, Saville M, Wood J, et al. Safety and immunogenicity of an inactivated split-virion influenza A/Vietnam/1194/2004 (H5N1) vaccine: phase I randomised trial. *Lancet* 2006;367(9523):1657–64.
- [7] Treanor JJ, Wilkinson BE, Masseoud F, Hu-Primmer J, Battaglia R, O'Brien D, et al. Safety and immunogenicity of a recombinant hemagglutinin vaccine for H5 influenza in humans. *Vaccine* 2001;19(13–14):1732–7.
- [8] Wright PF, Dolin R, La Montagne JR. From the National Institute of Allergy and Infectious Diseases of the National Institutes of Health, the Center for Disease Control, and the Bureau of Biologics of the Food and Drug Administration. Summary of clinical

- trials of influenza vaccines—II. *J Infect Dis* 1976;134(6):633–8.
- [9] Cate TR, Couch RB, Kasel JA, Six HR. Clinical trials of monovalent influenza A/New Jersey/76 virus vaccines in adults: reactivity, antibody response, and antibody persistence. *J Infect Dis* 1977;136(Suppl.):450–5.
- [10] Lin J, Zhang J, Dong X, Fang H, Chen J, Su N, et al. Safety and immunogenicity of an inactivated adjuvanted whole-virion influenza A (H5N1) vaccine: a phase I randomised controlled trial. *Lancet* 2006;368(9540):965–6.
- [11] Subbarao K, Luke C. H5N1 viruses and vaccines. *PLoS Pathog* 2007;3(3):e40.
- [12] Minimal Requirements for Biological Products, National Institute of Infectious Diseases Japan; 2006. See website <http://www.nih.go.jp/nid/IRBP/index-e.html>.
- [13] Kurokawa M, Ishida S, Asakawa S, Iwasa S, Goto N, Kuratsuka K. Toxicities of influenza vaccine: peripheral leukocytocrescence to live and inactivated influenza viruses in mice. *Jpn J Med Sci Biol* 1975;28:37–52.
- [14] Chino F. The views and policy of the Japanese control authorities on the three Rs. *Dev Biol Stand* 1996;86:53–62.
- [15] Authier FJ, Gherardi RK. Safety and immunogenicity of H5N1 vaccine. *Lancet* 2006;367(9523):1657–64.
- [16] Exley C. Aluminium-containing DTP vaccines. *Lancet Infect Dis* 2004;4:324 (Discussion 325).
- [17] Hamaguchi I, Imai J, Momose H, Kawamura M, Mizukami T, Kato H, et al. Two vaccine toxicity-related genes Agp and Hpx could prove useful for pertussis vaccine safety control. *Vaccine* 2007;25(17):3355–64.
- [18] Kobayashi S, Ito E, Honma R, Nojima Y, Shibuya M, Watanabe S, et al. Dynamic regulation of gene expression by the Flt-1 kinase and Matrigel in endothelial tubulogenesis. *Genomics* 2004;84(1):185–92.
- [19] Ito E, Honma R, Imai J, Azuma S, Kanno T, Mori S, et al. A tetraspanin-family protein, T-cell acute lymphoblastic leukemia-associated antigen 1, is induced by the Ewing's sarcoma-Wilms' tumor 1 fusion protein of desmoplastic small round-cell tumor. *Am J Pathol* 2003;163(6):2165–72.
- [20] Churchill GA. Fundamentals of experimental design for cDNA microarrays. *Nat Genet* 2002;32:490–5.
- [21] Ito E, Honma R, Yanagisawa Y, Imai J, Azuma S, Oyama T, et al. Novel clusters of highly expressed genes accompany genomic amplification in breast cancers. *FEBS Lett* 2007;581:3909–14.
- [22] Miura A, Honma R, Togashi T, Yanagisawa Y, Ito E, Imai J, et al. Differential responses of normal human coronary artery endothelial cells against multiple cytokines comparatively assessed by gene expression profiles. *FEBS Lett* 2006;580(30):6871–9.
- [23] Fujita N, Miyamoto T, Imai J, Hosogane N, Suzuki T, Yagi M, et al. CD24 is expressed specifically in the nucleus pulposus of intervertebral discs. *Biochem Biophys Res Commun* 2005;338(4):1890–6.
- [24] Sakamoto A, Imai J, Nishikawa A, Honma R, Ito E, Yanagisawa Y, et al. Influence of inhalation anesthesia assessed by comprehensive gene expression profiling. *Gene* 2005;356:39–48.
- [25] Shi L, Tong W, Fang H, Scherf U, Han J, Puri RK, et al. Cross-platform comparability of microarray technology: intra-platform consistency and appropriate data analysis procedures are essential. *BMC Bioinform* 2005;6(Suppl. 2):S12.
- [26] Haller O, Staeheli P, Kochs G. Interferon-induced Mx proteins in antiviral host defense. *Biochimie* 2007;89(6–7):812–8.
- [27] Baskin CR, Garcia-Sastre A, Tumpey TM, Bielefeldt-Ohmann H, Carter VS, Nistal-Villan E, et al. Integration of clinical data, pathology, and cDNA microarrays in influenza virus-infected pigtailed macaques (*Macaca nemestrina*). *J Virol* 2004;78(19):10420–32.
- [28] Kobasa D, Jones SM, Shinya K, Kash JC, Copps J, Ebihara H, et al. Aberrant innate immune response in lethal infection of macaques with the 1918 influenza virus. *Nature* 2007;445(7125):319–23.
- [29] Tong HH, Long JP, Li D, DeMaria TF. Alteration of gene expression in human middle ear epithelial cells induced by influenza A virus and its implication for the pathogenesis of otitis media. *Microb Pathog* 2004;37(4):193–204.
- [30] Ishiguro N, Takada A, Yoshioka M, Ma X, Kikuta H, Kida H, et al. Induction of interferon-inducible protein-10 and monokine induced by interferon-gamma from human endothelial cells infected with influenza A virus. *Arch Virol* 2004;149(1):17–34.
- [31] Mashima R, Saeki K, Aki D, Minoda Y, Takaki H, Sanada T, et al. FLN29, a novel interferon- and LPS-inducible gene acting as a negative regulator of toll-like receptor signaling. *J Biol Chem* 2005;280(50):41289–97.
- [32] Collazo CM, Yap GS, Sempowski GD, Lusby KC, Tessarollo L, Woude GF, et al. Inactivation of LRG-47 and IRG-47 reveals a family of interferon gamma-inducible genes with essential, pathogen-specific roles in resistance to infection. *J Exp Med* 2001;194(2):181–8.
- [33] Agostini C, Faccio M, Siviero M, Carollo D, Galvan S, Cattelan AM, et al. CXC chemokines IP-10 and mig expression and direct migration of pulmonary CD8+/CXCR3+ T cells in the lungs of patients with HIV infection and T-cell alveolitis. *Am J Respir Crit Care Med* 2000;162:1466–73.
- [34] Peiris JS, Yu WC, Leung CW, Cheung CY, Ng WF, Nicholls JM, et al. Re-emergence of fatal human influenza A subtype H5N1 disease. *Lancet* 2004;363(9409):617–9.
- [35] Tewari MK, Sinnathamby G, Rajagopal D, Eisenlohr LC. A cytosolic pathway for MHC class II-restricted antigen processing that is proteasome and TAP dependent. *Nat Immunol* 2005;6(3):287–94.
- [36] Uger RA, Chan SM, Barber BH. Covalent linkage to beta2-microglobulin enhances the MHC stability and antigenicity of suboptimal CTL epitopes. *J Immunol* 1999;162(10):6024–8.
- [37] Gueders MM, Foidart JM, Noel A, Cataldo DD. Matrix metalloproteinases (MMPs) and tissue inhibitors of MMPs in the respiratory tract: potential implications in asthma and other lung diseases. *Eur J Pharmacol* 2006;533:133–44.
- [38] Ichihara T, Morishima T, Kajimoto M, Matsushige T, Matsubara T, Furukawa S. Matrix metalloproteinase-9 and tissue inhibitors of metalloproteinases 1 in influenza-associated encephalopathy. *Pediatr Infect Dis J* 2007;26(6):542–4.
- [39] Ropper AH, Victor M. Influenza vaccination and the Guillain-Barre syndrome. *N Engl J Med* 1998;339(25):1845–6.
- [40] Souayah N, Nasar A, Suri MF, Qureshi AI. Guillain-Barre syndrome after vaccination in United States a report from the CDC/FDA Vaccine Adverse Event Reporting System. *Vaccine* 2007;25(29):5253–5.

Transcutaneous immunization by merely prolonging the duration of antigen presence on the skin of mice induces a potent antigen-specific antibody response even in the absence of an adjuvant

Seishiro Naito^{a,*}, Jun-ichi Maeyama^a, Takuo Mizukami^a, Motohide Takahashi^b,
Isao Hamaguchi^a, Kazunari Yamaguchi^a

^a Department of Safety Research on Blood and Biological Products, National Institute of Infectious Diseases, 4-7-1 Gakuen, Musashimurayama, Tokyo 208-0011, Japan

^b Department of Bacterial Pathogenesis and Infection Control, National Institute of Infectious Diseases, 4-7-1 Gakuen, Musashimurayama, Tokyo 208-0011, Japan

Received 25 April 2007; received in revised form 7 September 2007; accepted 12 October 2007

Available online 1 November 2007

Abstract

Transcutaneous immunization (TCI) is a promising needle-free technique for vaccination. In this method, strong adjuvants, such as the cholera toxin, are generally crucial to elicit a robust immune response. Here, we showed that prolonged antigen presence on the skin of mice during TCI could effectively enhance the immune response. Substantial antigen-specific antibodies were produced in the sera of mice even after non-adjuvanted TCI when the antigen presence was for longer than 16 h. This non-adjuvanted TCI method was applied using the tetanus toxoid, and potent tetanus toxoid-specific antibodies were successfully induced in the sera of mice; they survived a lethal tetanus toxin challenge with no clinical signs. Thus, non-adjuvanted approach might be a possible option for TCI, and this method might improve the safety and practicality of transcutaneous vaccination.

© 2007 Elsevier Ltd. All rights reserved.

Keywords: Transcutaneous immunization; Adjuvant; Tetanus toxoid

1. Introduction

The skin is one of the first lines of defense of the body. During the course of evolution, the skin has developed a dense immune system comprising draining lymph nodes and various immunocompetent cells such as Langerhans cells, keratinocytes, dermal dendritic cells, and mast cells [1,2]. Together with its high accessibility, the skin's immunocompetence makes it an ideal target for vaccination.

Recently, there have been reports of needle-free vaccinations that target the intact skin surface and use peptides, proteins, or virus particles as antigens [3–7]. These novel methods, referred to as transcutaneous immunization (TCI),

are performed by the topical application of antigens along with adjuvants. It is generally considered that some amount of a potent adjuvant is crucial in order to elicit a robust immune response against antigens co-administered via skin delivery [8,9]. The most common adjuvants used in the TCI method are the cholera toxin (CT) or the heat-labile enterotoxin (LT) from *Escherichia coli* [10].

Needle-free vaccination methods are desirable because they are convenient, painless, and relatively safe. In particular, vaccinations in developing countries and mass vaccinations against expected pandemics would benefit greatly from needle-free approaches [11]. Although TCI is a promising needle-free approach, the indispensable use of potent bacterial toxins as adjuvants might raise some concerns regarding the safety of this method; however, CT and LT may be less toxic when applied on the skin surface [12].

* Corresponding author. Tel.: +81 42 561 0771; fax: +81 42 565 3315.
E-mail address: snaito@nih.go.jp (S. Naito).

In this study, we merely prolonged the duration of antigen presence on the skin of mice during the TCI procedure and observed that the serum antibody titre increased in a duration-dependent manner. We induced substantial serum antibody responses by a TCI of 16-h duration even in the absence of an adjuvant. In this report, we applied a modified TCI method termed "prolonged TCI" that involved no adjuvant. In this method, the tetanus toxoid (Ttd) was used as a model vaccine antigen, and this method successfully induced potent tetanus toxoid-specific antibody responses in the sera of mice; these mice survived a lethal tetanus toxin challenge without any clinical signs. These results indicate that the non-adjuvanted approach might be a possible option for TCI. This might improve the safety and practicality of transcutaneous vaccination.

2. Materials and Methods

2.1. Mice

We used female C57BL/6, BALB/c, and C3H/He mice (Japan SLC Inc., Hamamatsu, Japan) aged 7–8 weeks at the primary immunizations.

The animals were housed in a specific pathogen-free facility and provided with free access to water and food. The use of the animals and the study protocols were approved by the institutional animal care and use committee.

2.2. Antigens and adjuvant

Ovalbumin (OVA) and CT were purchased from Sigma (St. Louis, MO, USA). The Ttd was kindly provided by Kaketsuken (Kumamoto, Japan).

2.3. Conventional TCI

Conventional TCI was performed as previously described [10]. In brief, the abdomen of the mice was shaved using a No. 40 clipper, and the mice were rested for 48 h. They were anaesthetized intraperitoneally with a ketamine–xylazine mixture to prevent self-grooming. The bare abdominal skin was gently swabbed with 70% ethanol and allowed to dry. Next, 50 μ l of antigen solution in PBS was placed on the bare abdominal skin over an approximate area of 1 cm² for 2 h. The mice were then washed extensively with lukewarm tap water and patted dry with paper towels.

2.4. Prolonged TCI

Mice were shaved and anaesthetized in the same manner as that used for the conventional TCI. The bare abdominal skin was gently swabbed with 70% ethanol and allowed to dry. Next, a 0.64-cm² square gauze patch with an adhesive lining (Shirojuhji, Tokyo, Japan) was soaked with 50 μ l of antigen solution, and was fixed to the bare abdominal skin

using medical tape (Fig. 1A and C). The mice were placed back in the cage and left for 16 h or more. Then, the medical tape and gauze patch were removed, and the abdominal skin was extensively washed with lukewarm tap water and patted dry with paper towels.

Prolonged TCI of the dorsal side of the ear was performed as described above without shaving (Fig. 1B and D).

2.5. Fecal extract

Fecal samples were collected and weighed. A hundred milligram of feces were suspended in 400 μ l of PBS containing 100 μ g/ml of soybean trypsin inhibitor (Wako, Ohsaka, Japan), 50 mM of EDTA, 1 mM of phenylmethylsulfonyl fluoride (Sigma), 1% of bovine serum albumin (Sigma), 5% of fetal bovine serum (Sigma), and 0.05% of sodium azide, were vigorously vortexed to homogeneity, centrifuged at 6000 \times g for 5 min and the supernatants were collected and stored at -20° C until assayed.

2.6. ELISA for antigen-specific IgG and IgA antibodies

Antigen-specific IgG and IgA antibody titres of the sera and fecal extracts were determined by ELISA. In brief, 96-well plates (MaxiSorp; Nunc, Roskilde, Denmark) were coated with antigen in 0.1 M carbonate/bicarbonate buffers, pH 9.0, and blocked with PBS containing 1% bovine serum albumin (Sigma). After blocking, serial dilutions of the serum samples or fecal extracts were added to the plates, which were incubated at room temperature for 1.5 h. The plates were washed 3 times with wash buffer (PBS containing 0.05% Tween 20), and peroxidase-labeled rabbit anti-mouse IgG antibodies (Zymed, San Francisco, CA, USA) or peroxidase-labeled goat anti-mouse IgA antibodies (Zymed) were added. After 1.5-h incubation at room temperature, the plates were washed 3 times with the wash buffer, and *o*-phenylenediamine (Sigma) in phosphate/citrate buffer containing 0.03% H₂O₂ was added. The reactions were arrested 10 min later by adding 1 N H₂SO₄, and optical densities were measured at 492 nm. Endpoint titres were expressed as reciprocal log₂ of the limit dilutions that recorded an optical density greater than 1.0.

2.7. Tetanus toxin challenge

The left hind thigh of the mice was injected subcutaneously with 10 median lethal dose (LD₅₀) of tetanus toxin in 0.5 ml PBS, and the mice were observed daily for up to 7 days. The mice that developed severe paralysis were euthanized.

2.8. Statistical analysis

The data are represented as the geometric means of the values obtained from individual animals. The groups were compared using unpaired two-tailed Student's *t*-tests, and *p*-values ≤ 0.05 were regarded as significant.

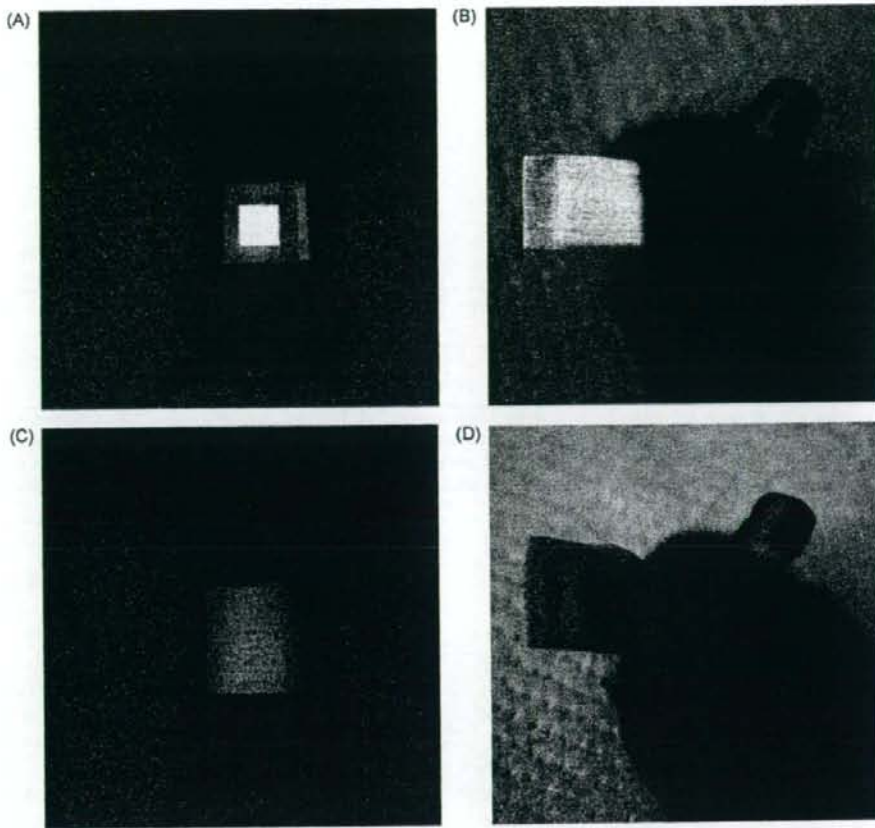


Fig. 1. Prolonged TCI using gauze patch. The gauze patch soaked with 50 μ l of antigen solution was applied to the bare abdominal skin (A) or the dorsal side of the ear skin (B), and fixed with medical tape (C, D).

3. Results

3.1. Conventional TCI induced a substantial antigen-specific serum antibody response; however, the use of an adjuvant was crucial

We confirmed the crucial roll of CT as an adjuvant in the conventional TCI method.

The C57BL/6 mice were immunized by the conventional TCI procedure with 100 μ g of OVA with or without 10 μ g of CT as an adjuvant. Another group of mice was injected intradermally with an identical dose of OVA solution without CT. They were immunized in an identical manner 3 times with 2-week intervals. At 2 weeks after the last immunization, we collected serum samples and determined the OVA-specific and CT-specific IgG antibody titres by ELISA. When an adjuvant was used, as in the conventional TCI, we observed that the level of OVA-specific IgG antibodies induced was comparable to that induced by the intradermally injected OVA solution (Fig. 2A). CT-

specific IgG antibody responses were also induced by the adjuvanted TCI (Fig. 2B). In contrast, the non-adjuvanted conventional TCI induced no significant serum antibody response.

3.2. Prolonged TCI induced a substantial antigen-specific serum antibody response even in the absence of an adjuvant

We examined the effect of prolongation of the duration of antigen presence on the skin to the immune response induced by TCI.

The bare abdominal skin or the dorsal side of the ears of the C57BL/6 mice were immunized with 100 μ g of OVA with or without 10 μ g of CT as an adjuvant according to the prolonged TCI procedure; the duration of the patch immunizations varied from 2 to 32 h. Booster immunizations were performed in an identical manner 2 times with 2-week intervals. At 2 weeks after the last immunization, we collected serum samples from the mice and determined their OVA-

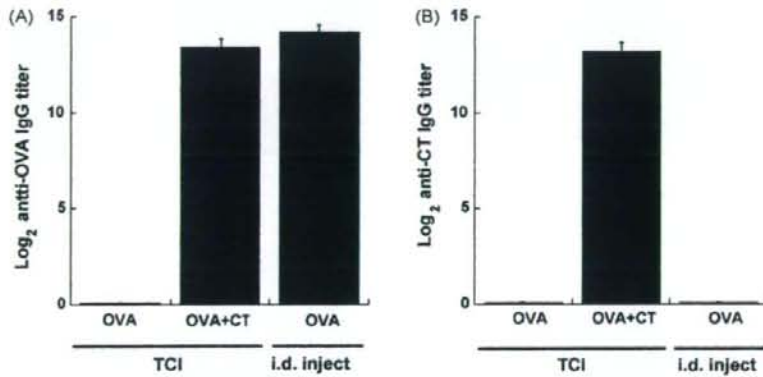


Fig. 2. Antigen- or adjuvant-specific serum IgG antibody response after conventional TCI. The bare abdominal skin of C57BL/6 mice ($n=5$) was applied directly with 50 μ l of OVA solution (2 mg/ml) with or without CT (200 μ g/ml) as an adjuvant for 2 h. Another group of mice ($n=5$) was injected intradermally with an identical dose of OVA solution without CT. Immunizations were performed in an identical manner for each group of mice at 0, 2, and 4 weeks. OVA-specific (A) or CT-specific (B) IgG titres in the serum samples were determined at 6 weeks after the primary immunization. The geometric means and the standard error of the means are shown for each group.

specific IgG antibody titres. The 2-h patch immunization with an adjuvant to the abdomen induced substantial OVA-specific serum IgG antibody production, while the 2-h immunization without an adjuvant did not induce a significant antibody response. However, the 16-h patch immunization without an adjuvant also induced a significant antibody response (Fig. 3A). On the other hand, the 2-h patch immunization of the ear induced a significant antibody response even without an adjuvant, and the titres of serum OVA-specific IgG antibodies increased with the duration of the patch immunization. The antibody titres produced by the non-adjuvanted 16-h and 32-h patch immunizations of the ear were comparable to that produced by the adjuvanted 2-h patch

immunization (Fig. 3B). Thus, the prolonged TCI with patch immunization for greater than 16 h induced a substantial antigen-specific serum antibody response even when it was non-adjuvanted.

Next, we compared the immunization to the bare abdominal skin with that to the dorsal side of the ear skin for determining the most suitable target site for the prolonged TCI.

C57BL/6 mice were immunized using the prolonged TCI procedure with 10 or 100 μ g of OVA without an adjuvant. We boosted the mice 2 times at 2-week intervals using the same manner of immunization as that used for the primary TCI and determined the OVA-specific serum IgG antibody titres

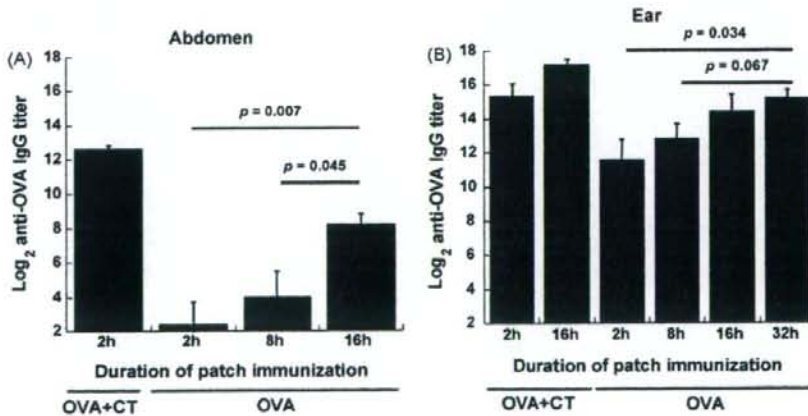


Fig. 3. Prolonged antigen presence on the skin. Gauze patches soaked with 50 μ l of OVA solutions (2 mg/ml) with or without CT (200 μ g/ml) as an adjuvant were taped to the bare abdominal skins (A) or the dorsal side of the left ears (B) of C57BL/6 mice ($n=5$) for 2, 8, 16, or 32 h. Immunizations for each group of mice were performed in an identical manner at 0, 2, and 4 weeks. OVA-specific IgG titres in serum samples were determined at 6 weeks after the primary immunization. The geometric means and the standard error of the means are shown for each group.

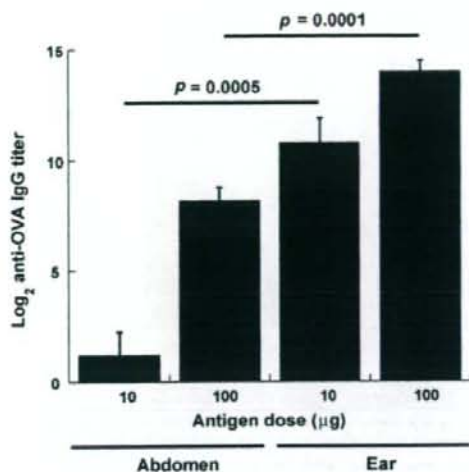


Fig. 4. Comparison between the abdominal skin and the ear skin for determining the most suitable target site for prolonged TCI. The bare abdominal skins or the dorsal side of the left ears of C57BL/6 mice ($n = 5$) were immunized by non-adjuvanted prolonged TCI procedure with 10 or 100 µg of OVA for 16 h. Immunization of each group of mice was performed in an identical manner at 0, 2, and 4 weeks. OVA-specific IgG titres in serum samples were determined at 6 weeks after the primary immunization. The geometric means and the standard error of the means are shown for each group.

2 weeks after the last immunization. We found that, with both doses of OVA, the immunization of the dorsal sides of ears induced higher titres of antibodies than that of the bare abdominal skin (Fig. 4). Thus, the prolonged TCI procedure immunized the ear skin more efficiently than the abdominal skin.

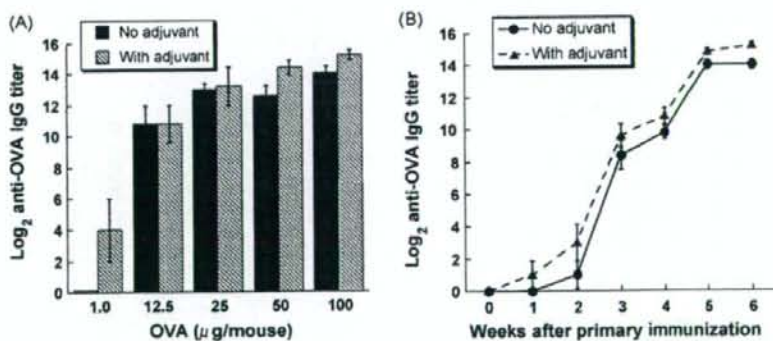


Fig. 5. Dose-response (A) and time-course (B) of serum antibody production by the non-adjuvanted or adjuvanted prolonged TCI procedure. (A) The ears of C57BL/6 mice ($n = 5$) were immunized by prolonged TCI procedure for 16 h with the indicated doses of OVA from 1.0 to 100 µg with (hatched bars) or without (solid bars) 10 µg of CT as an adjuvant. Each group of mice was immunized in an identical manner at 0, 2, and 4 weeks. OVA-specific IgG titres in serum samples were determined at 6 weeks after the primary immunization using ELISA. The geometric mean and the standard error of the mean are shown for each group. (B) The ears of C57BL/6 mice ($n = 5$) were immunized by the prolonged TCI procedure for 16 h with 100 µg of OVA with (closed triangles and a broken line) or without (closed circles and an unbroken line) 10 µg of CT as an adjuvant at 0, 2, and 4 weeks. OVA-specific IgG titres in serum samples were determined every week up to 6 weeks after the primary immunization. The geometric means and the standard error of the means are shown for each group and time.

3.3. Non-adjuvanted prolonged TCI of the ear skin induced a serum antibody response comparable induced by the adjuvanted TCI

We compared the serum antibody responses induced by the non-adjuvanted prolonged TCI and adjuvanted TCI by using dose-response and time-course studies.

Patches containing 1.0, 12.5, 25, 50, or 100 µg of OVA and with or without 10 µg of CT were taped to the dorsal side of the ears of the C57BL/6 mice for 16 h according to the prolonged TCI procedure. We boosted the mice twice with 2-week intervals in a manner identical to that used for the primary immunization and determined the serum OVA-specific IgG antibody titres 2 weeks after the last immunization. The titres of the serum IgG antibodies increased in a dose-dependent manner, and there was no significant difference between the magnitudes of the serum antibody response induced by the non-adjuvanted prolonged TCI and that induced by the adjuvanted TCI (Fig. 5A).

In the time-course experiment, we immunized the ears of the C57BL/6 mice with 100 µg of OVA with or without 10 µg of CT according to the prolonged TCI procedure and boosted the mice twice at 2-week intervals in a manner identical to that used for the primary immunization. We collected serum samples prior to the immunization and every week for 1–6 weeks after the primary immunization. Further, we determined the time-course of the OVA-specific IgG antibody productions. Significant serum anti-OVA antibody production was observed after the first booster immunization, and this production was enhanced by the second booster immunization. There were no significant differences between the serum antibody responses induced by the non-adjuvanted prolonged TCI and the adjuvanted one, except with regard to

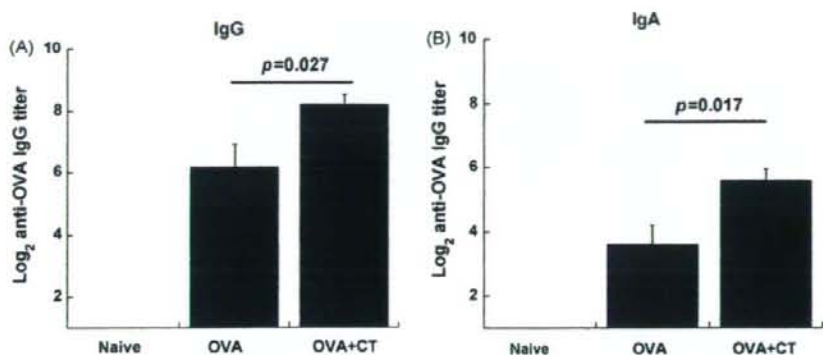


Fig. 6. Fecal antibody responses induced by the non-adjuvanted or adjuvanted prolonged TCI procedure. The ears of C57BL/6 mice ($n=5$) were immunized by prolonged TCI procedure for 16 h with 100 μg of OVA with or without 10 μg of CT as an adjuvant at 0, 2, and 4 weeks. Another group of mice ($n=5$) was inoculated nothing as a negative control. The fecal samples were collected at 6 weeks after the primary immunization and OVA-specific IgG (A) and IgA (B) titers in the fecal extracts were determined. The geometric means and the standard error of the means are shown for each group.

the antibody titres at 6 weeks after the primary immunization (Fig. 5B).

Thus, the non-adjuvanted prolonged TCI comprising the 16-h antigen presence induced serum antigen-specific antibody responses of a level comparable to that observed with the adjuvanted TCI.

3.4. Non-adjuvanted prolonged TCI induced significant fecal antibody responses

Previous studies demonstrated that CT-adjuvanted TCI elicited not only systemic but also mucosal antibody responses. We examined the fecal IgG and IgA antibody responses after adjuvanted and non-adjuvanted TCI.

Patches containing 100 μg of OVA and with or without 10 μg of CT were applied to the dorsal side of the ears of the C57BL/6 mice for 16 h. We boosted the mice twice with 2-week intervals in a manner identical to that used for the primary immunization. Other group of mice were inoculated nothing as a negative control. We collected the fecal samples at 2 weeks after the last immunization.

Both groups of the immunized mice produced significant fecal IgG and IgA antibodies (Fig. 6). The CT-adjuvanted TCI group indicated approximately 4-fold higher titers of antibody production than the non-adjuvanted group.

3.5. Non-adjuvanted prolonged TCI of the ear skin induced a significant serum antibody response, regardless of mice strains

We examined strain differences with regard to the serum antibody responses induced by the prolonged TCI procedure. The ears of the C57BL/6, BALB/c, or C3H/He mice were immunized with 100 μg of OVA with or without 10 μg of CT according to the prolonged TCI procedure. The mice were boosted twice at 2-week intervals, and

the OVA-specific IgG antibody production in their sera was determined 2 weeks after the last immunization. We observed significant differences in the magnitude of the serum OVA-specific IgG antibody responses among the different strains of mice. Among the 3 strains, the C57BL/6 mice produced the highest amounts of serum antigen-specific IgG antibodies, while the C3H/He mice produced the least amounts. Besides, both the non-adjuvanted prolonged TCI and the adjuvanted one induced substantial serum antibody responses in all the strains of mice that were examined (Fig. 7).

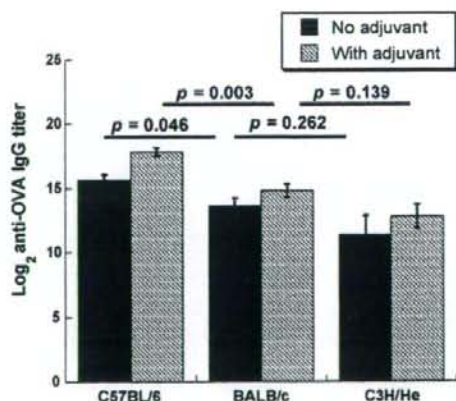


Fig. 7. Differences between the mice strains with regard to the serum antigen-specific IgG responses induced by the non-adjuvanted or adjuvanted prolonged TCI procedure. The ears of C57BL/6 ($n=5$), BALB/c ($n=5$), or C3H/He ($n=5$) mice were immunized with 100 μg of OVA with (hatched bars) or without (solid bars) 10 μg of CT as an adjuvant according to the prolonged TCI procedure for 16 h at 0, 2, and 4 weeks. OVA-specific IgG titers in serum samples were determined at 6 weeks after the primary immunization. The geometric means and the standard error of the means are shown for each group.

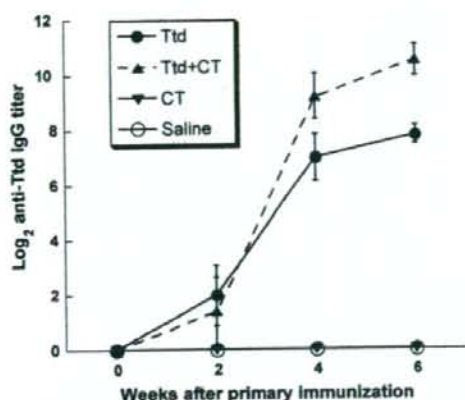


Fig. 8. Immunization using the tetanus toxoid (Ttd) for the prolonged TCI procedure with or without adjuvant. The ears of C57BL/6 mice ($n=5$, but $n=4$ for the "with adjuvant" group) were immunized by the prolonged TCI procedure for 16 h with 10 Lf of Ttd with (closed triangles and a broken line) or without (closed circles and an unbroken line) 10 μ g of CT as an adjuvant at 0, 2, and 4 weeks. The negative controls were immunized with 10 μ g of CT (reverse closed triangles and an unbroken line) or vehicle (PBS) alone (open circles and an unbroken line) in an identical manner. OVA-specific IgG titres in serum samples were determined every 2 weeks for up to 6 weeks after the primary immunization. The geometric means and the standard error of the means are shown for each group and time.

3.6. Prolonged TCI using the Ttd induced a robust antibody response and provided protection against tetanus toxin challenge

We immunized the ears of the C57BL/6 mice with 10 flocculation units (Lf) of Ttd with or without 10 μ g of CT according to the prolonged TCI procedure. As controls, we also immunized another group of mice with 10 μ g of CT or vehicle (PBS) alone. We boosted the mice twice at 2-week intervals in a manner identical to that used for the primary immunization. We collected serum samples every alternate week for up to 6 weeks after the primary immunization and determined the titres of Ttd-specific IgG antibodies in the sera. Regardless of the use of the adjuvant, significant levels of Ttd-specific IgG antibodies were induced in the sera of the mice immunized with the Ttd, and these levels increased after the booster immunizations (Fig. 8). In contrast, in the mice immunized with either the CT or vehicle

Table 1
Tetanus toxin challenge^a

	Survival/total	% Survival
Saline	0/5	0
CT	0/5	0
Ttd	5/5	100
Ttd + CT	4/4	100

^a C57BL/6 mice were immunized by prolonged TCI procedure with 10 Lf of Ttd with or without 10 μ g of CT at 0, 2, 4 weeks. Ten micrograms of CT or vehicle (saline) alone were immunized to the other groups of mice by the same way. Ten LD₅₀ of tetanus toxins were challenged at 7 weeks after primary immunization.

alone, no Ttd-specific IgG antibodies were induced at all the times examined.

Next, we challenged these mice with a lethal dose of tetanus toxin at 7 weeks after the primary immunization. All the control mice (only CT or vehicle immunized) died within 2 days of the challenge with signs of tetanus (Table 1). In contrast, all the mice immunized with the Ttd survived and demonstrated no clinical signs regardless of adjuvant use.

4. Discussion

In the recent decade, many studies have demonstrated the feasibility of TCI using various antigens [3–7], adjuvants [10,13–16], skin treatments [7,17–19], and animals [20–24]. Under these various settings, most experiments followed a protocol in which antigens were topically applied for 1–2 h and reported the critical role of adjuvants for the induction of robust immune responses. Skin pretreatments such as skin abrasion [25], application of penetration enhancers [7,26], use of electrophoresis [17] or sonophoresis [18] techniques, and the use of lipid carriers [20,27] were applied in some experiments; these pretreatments might promote antigen penetration through the skin. Overall, some potent adjuvants and/or some skin penetration-enhancing methods are believed to be necessary to induce robust immune responses by TCI. Nevertheless, a few papers [28–30] reported that substantial immune responses were successfully induced in the absence of any adjuvants or penetration-enhancing methods. Further, in all of these experiments, the antigens were applied topically for a comparatively long-period of above overnight. These results suggest that the duration of antigen presence on the skin during the TCI procedure might be an important parameter affecting the magnitude of the immune responses. However, thus far, the relationship between the duration of antigen presence on the skin and the magnitude of the immune response remains to be clearly elucidated. In this report, we applied OVA as an antigen for varying durations of 2–32 h on the intact skin of mice and observed that if the antigen was present on the skin for a prolonged duration, the serum antibody response was enhanced in a duration-dependent manner. Surprisingly, patch immunization on intact skin for above 16 h (referred to as prolonged TCI in this paper) induced substantial serum antibody responses even in the absence of any adjuvants. Dose–response and time-course experiments revealed that non-adjuvanted prolonged TCI to the mice ear induced serum antibody responses comparable in magnitude to those induced by adjuvanted prolonged TCI. Thus, our observations clearly indicated that the duration of antigen presence on the skin is an important factor influencing the effectiveness of TCI.

Several reports assume that some danger signals from bacterial adjuvants are necessary to activate Langerhans cells and trigger immune responses [8]. However, our data indicate that additional adjuvants are not prerequisites for the induction of immune responses. This result might imply that the antigen